AD_____

Award Number: W81XWH-10-1-0292

TITLE: T-Pharmacytes for Prostate Cancer Immunotherapy

PRINCIPAL INVESTIGATOR: Jianzhu Chen

CONTRACTING ORGANIZATION: Massachusetts Institute of Technology
Cambridge, MA 02139-4301

REPORT DATE: June 2013

TYPE OF REPORT: Final Report

PREPARED FOR: U.S. Army Medical Research and Materiel Command
Fort Detrick, Maryland 21702-5012

DISTRIBUTION STATEMENT: Approved for Public Release;
Distribution Unlimited

REPORT DOCUMENTATION PAGE

Form Approved
OMB No. 0704-0188

1. REPORT DATE	2. REPORT TYPE	3. DATES COVERED
June 2013	Final	15 May 2010 – 14 May 2013

4. TITLE AND SUBTITLE
T-Pharmacytes for Prostate Cancer Immunotherapy

5a. CONTRACT NUMBER

5b. GRANT NUMBER
W81XWH-10-1-0292

5c. PROGRAM ELEMENT NUMBER

6. AUTHOR(S)

Jianzhu Chen, S. Peter Bak, Michael Barnkob, Ailin Bai, Eileen Higham, & K. Dane Wittrup,

E-Mail: jchen@mit.edu

5d. PROJECT NUMBER

5e. TASK NUMBER

5f. WORK UNIT NUMBER

7. PERFORMING ORGANIZATION NAME(S) AND ADDRESS(ES)
Massachusetts Institute of Technology
Cambridge, MA 02139-4301

8. PERFORMING ORGANIZATION REPORT NUMBER

9. SPONSORING / MONITORING AGENCY NAME(S) AND ADDRESS(ES)
U.S. Army Medical Research and Materiel Command
Fort Detrick, Maryland 21702-5012

10. SPONSOR/MONITOR'S ACRONYM(S)

11. SPONSOR/MONITOR'S REPORT NUMBER(S)

12. DISTRIBUTION / AVAILABILITY STATEMENT
Approved for Public Release; Distribution Unlimited

13. SUPPLEMENTARY NOTES

14. ABSTRACT

Adoptive cell therapy (ACT) of cancer with *ex vivo* activated/expanded T-cells is one of the promising treatments currently being tested in patients. One challenge of the approach is that the transferred T cells become functionally anergic in the tumor environment, limiting their anti-tumor effect. We have investigated whether tumor-mediated immune suppression can be overcome by arming tumor-specific T cells with cytokine/immunostimulator-loaded nanoparticles carried by each cell. Specially, we have defined the role of CD70 and CD80/CD86 in dendritic cell-mediated activation of tumor tolerized CD8 T cells, discovered the effect of CD8 T cell responses in selecting for antigen-negative tumor cells, and develop a better prostate model for monitoring T cell responses to prostate cancer in mice. Findings from our studies identify molecular interactions that are important for maintaining T cell function in the tumor environment, suggesting possible interventions to enhance T cell functionality during ACT. Our results that CD8 T cells are effective in eliminating antigen-bearing prostate tumor cells but they also can select for the outgrowth of antigen-negative tumor cells provide insights into the requirements for an effective cancer immunotherapy: not only inducing potent immune responses but also avoiding selection and outgrowth of antigen-negative tumor cells.

15. SUBJECT TERMS
Adoptive cell therapy, immunotherapy, prostate, tolerance, tumor-infiltrating lymphocytes

16. SECURITY CLASSIFICATION OF:			17. LIMITATION OF ABSTRACT	18. NUMBER OF PAGES	19a. NAME OF RESPONSIBLE PERSON
a. REPORT	b. ABSTRACT	c. THIS PAGE			USAMRMC
U	U	U	UU	48	19b. TELEPHONE NUMBER *(include area code)*

Table of Contents

Introduction

Adoptive cell therapy (ACT) of cancer with *ex vivo* activated/expanded T-cells is one of the promising treatments currently being tested in patients. One challenge of the approach is that the transferred T cells become functionally anergic in the tumor environment, limiting their anti-tumor effect (Rosenberg et al 2008, June 2007). The overall objective of our grant proposal is to test whether tumor-mediated immune suppression can be overcome by arming tumor-specific T cells with cytokine/immunostimulator-loaded nanoparticles carried by each cell. Specifically, we proposed the following three aims: 1) to optimize biodegradable 'lipid-enveloped' nanoparticles as cell surface drug carriers, 2) characterize the impact of T-cell surface-bound cytokine-NPs on T-cell proliferation, activation/target cell killing, and migration, and 3) measure T-cell tissue homing and biological responses triggered by cytokine-nanoparticle-carrying T-cells.

Body

In this Synergistic Idea Development Award, the Chen group has been contributing to Specific Aim #3: Measuring T-cell response in the prostate. In this aim we proposed to assess the *in vivo* functional effect of nanoparticles on T-cell trafficking and functions, and effects on the outcome for prostate tumors. The TRP-SIY model, which expresses a defined T-cell epitope, the SIY peptide, recognized by CD8 T cells expressing the 2C TCR, were used as a spontaneous prostate cancer model for these studies. By carrying out adoptive transfer experiments using 2C T-cells that recognize the SIY peptide expressed by the tumor, we can track a defined antigen-specific anti-tumor response. Primed 2C T-cells were used as the carrier of the therapeutic particles, mimicking the situation in human adoptive therapy treatments. The research progress from the Chen group is summarized below.

In study associated with Task 3.1 and 3.3, we investigated the role of co-stimulatory molecules in regulating functionality of tumor infiltrating CD8 T cells in the prostate. A major obstacle to efficacious T cell-based cancer immunotherapy is the tolerizing tumor microenvironment that rapidly inactivates tumor-infiltrating lymphocytes. We have previously developed an autochthonous model of prostate cancer by introducing 2C T cell epitope into the TRAMP transgenic mice (TRP-SIY) (Bai et al, 2008). In the TRP-SIY model, we have shown that intratumoral injection of antigen loaded dendritic cells (DCs) delays T cell tolerance induction as well as refunctionalizes already tolerized T cells in the tumor tissue (Higham et al 2010). In the current study, we have defined the molecular interactions that mediate DCs' effects (Bak et al, 2012).

We first investigated whether PD-1 and PD-L1 interaction is involved in the tolerization of transferred 2C T cells in the TRP-SIY mice as PD-1/PD-L1 interaction is one of the

major negative regulator of T cell function (Fife et al, 2008). By flow cytometry and histological staining, we show that PD-1 is expressed by T cells 6 days following infiltration into the prostate tumor tissue and that PD-L1 is expressed by prostate cells (Bak et al, 2012). To directly test the involvement of PD-1 and PD-L1, we generated TRP-SIY mice on a PD-L1$^{-/-}$ background. Following adoptive transfer of 2C T cells and intranasal infection with WSN-SIY influenza virus, effector 2C T cells infiltrated the prostate tumor tissue of TRP-SIY PD-L1$^{-/-}$ mice but rapidly lost IFN-γ expression, comparable to 2C T cells in prostates of TRP-SIY mice heterozygous for PD-L1 (Figure 1A), suggesting that PD-L1 is not required for T cell tolerance induction in the prostate tumor tissue of TRP-SIY mice.

To test whether the expression of PD-1 on 2C T cells could affect the subsequent function of T cells, we transferred 2C T cells into TRP-SIY mice and activated them by intranasal WSN-SIY infection. Seven days later, as newly induced effector 2C T cells entered the prostate, SIY-loaded bone marrow derived DCs (BMDCs) from wild type or PD-L1$^{-/-}$ mice were injected directly into the prostate tumor tissue to test if they delay the tolerance induction (Figure 1*B*). 2C T cells were recovered from the prostate another 6 days later and analyzed for their ability to express IFN-γ. Intraprostatic injection of SIY-loaded wild type or PD-L1$^{-/-}$ BMDCs stimulated similar percentages of 2C T cells to express IFN-γ when compared to PBS control (Figure 1*C*, 1*D*). Furthermore, 30 days after initial T cell transfer and infection, when infiltrating 2C T cells were already tolerized, SIY-loaded BMDCs from wild type or PD-L1$^{-/-}$ mice were injected intraprostatically to assess whether they reactivate the tolerized T cell *in situ* to a similar extent (Figure 1*B*). Intraprostatic injection of SIY-loaded wild type or PD-L1$^{-/-}$ BMDCs reactivated similar percentages of 2C T cells to express IFN-γ as compared to PBS control (Figure 1*C* and 1*E*). These data suggests that despite expression of PD-1 on 2C T cells and PD-L1 in the prostate tissue, disruption of PD-1/PD-L1 interaction does not enhance DC-mediated delay of tolerance induction or refunctionalization of already tolerized T cells in the prostate tumor tissue.

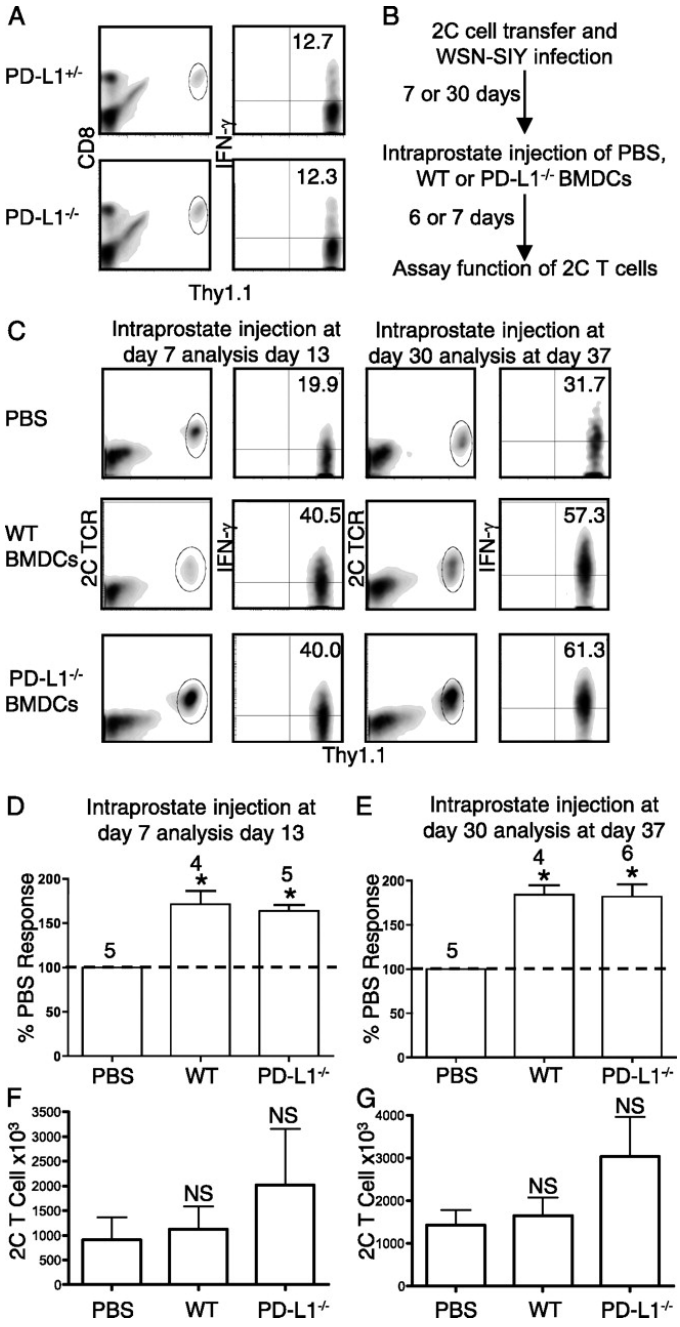

Figure 1. Modulation of the PD-1/PD-L1 interaction between 2C T cells and prostate or BMDCs does not affect T cell activity. (A) Naïve 2C T cells were transferred into PD-L1$^{+/-}$ or PD-L1$^{-/-}$ TRP-SIY mice along with intranasal infection with WSN-SIY virus. On day 14 2C T cells were harvested from prostate tissue, stimulated with SIY peptide and analyzed for IFN-γ expression. CD8 versus Thy1.1 plots were gated on all live cells from prostate. IFN-γ versus Thy1.1 plots were gated on CD8^{+} Thy1.1^{+} cells. Representative FACS plots from three experiments are shown. (B) Experimental scheme for analyzing BMDC-mediated delay of tolerance induction and refunctionalization of tolerized 2C cells in the prostate of TRP-SIY mice. On day 0, naïve 2C T cells were adoptively transferred into TRP-SIY mice and given intranasal infection with WSN-SIY virus. On day 7 or 30, mice were injected intraprostatically with PBS or 1x10^{6} *ex vivo* matured SIY-loaded wild type (WT) or PD-L1$^{-/-}$ BMDCs. Six to seven days later, 2C T cells were harvested from prostate tissue, stimulated with SIY peptide and analyzed for IFN-γ expression. (C) Representative plots of flow cytometry analyses of cells from prostate tissues of mice that were injected with PBS, wild type (WT), or PD-L1$^{-/-}$ BMDCs on either day 7 or day 30 after initial 2C cell transfer. 2C TCR versus Thy1.1 plots were gated on all live cells from prostate. IFN-γ versus Thy1.1 staining were gated on 2C TCR^{+} Thy1.1^{+} cells. The numbers indicate percentage of IFNγ^{+} cells. (D and E) Percentages (mean ± standard deviation) of IFN-γ^{+} 2C cells from three independent experiments normalized to PBS control. Number of mice for each treatment are indicated. * p<0.05 comparing DC versus PBS injection. (F and G) Number of 2C TCR^{+}Thy1.1^{+} cells from prostates injected with PBS, WT, or PD-L1$^{-/-}$ BMDCs either 7 (F) or 30 days (G) post T cells transfer and analyzed after 6 (F) or 7 days (G) later. Graphs are from three independent experiments with at least 4 mice per group. NS- no significance as compared to PBS control.

Next, we determined cell surface molecules on BMDCs that are required for reactivating 2C T cells in addition to SIY/MHC. Upregulated upon maturation of DCs, CD80 and CD86 provide an important stimulus in the context of the TCR/peptide MHC-1 engagement (Sharpe, 2009). Therefore, we compared the effect of intraprostatic injection of SIY-loaded wild type DC and DCs deficient in CD80, CD86, or both CD80 and CD86 in TRP-SIY mice. Compared to PBS injected mice, injection of SIY-loaded wild type BMDCs stimulated 2C T cells to express IFN-γ (Figure 2*B*). Surprisingly, intraprostatic injection of BMDCs from $CD80^{-/-}$, $CD86^{-/-}$, or $CD80^{-/-}CD86^{-/-}$ mice prolonged IFN-γ expression of infiltrating 2C T cells to a comparable extent, suggesting that neither CD80 nor CD86 is required for DC-mediated delay of tolerance induction in prostate tumor tissue.

In addition to their importance in T cell primary responses, CD80 and CD86 are important for simulating productive secondary responses (Fuse et al, 2008; HAbib-Agahi et al, 2007). To determine the requirement for CD80 and/or CD86 in DC-mediated refunctionalization of persisting tolerized T cells in the prostate tumor tissue, we injected SIY-loaded DCs from wild type, $CD80^{-/-}$, $CD86^{-/-}$, or $CD80^{-/-}CD86^{-/-}$ mice 30 days post initial 2C cell transfer and WSN-SIY infection. Intraprostatic injection of SIY-loaded wild type BMDCs reactivated tolerized T cells to express IFN-γ as compared to PBS control (Figure 2*C*). While injection of SIY-loaded $CD86^{-/-}$ BMDCs stimulated similar percentage of 2C cells to express IFN-γ in the prostate tumor tissue, the percentage of 2C cells that was induced to express IFN-γ was significantly reduced following injection of SIY-loaded $CD80^{-/-}$ BMDCs. Most dramatically, the ability of SIY-loaded BMDCs to induce 2C cell expression of IFN-γ was completely abrogated by deficiency of CD80 and CD86 (Figure 2D). These results suggest that although deficiency of CD86 can be compensated by the presence of CD80, CD80 deficiency cannot be completely compensated by the presence of CD86. Thus, CD80 is critically required for DC-mediated refunctionalization of tolerized T cells in the prostate tumor tissue.

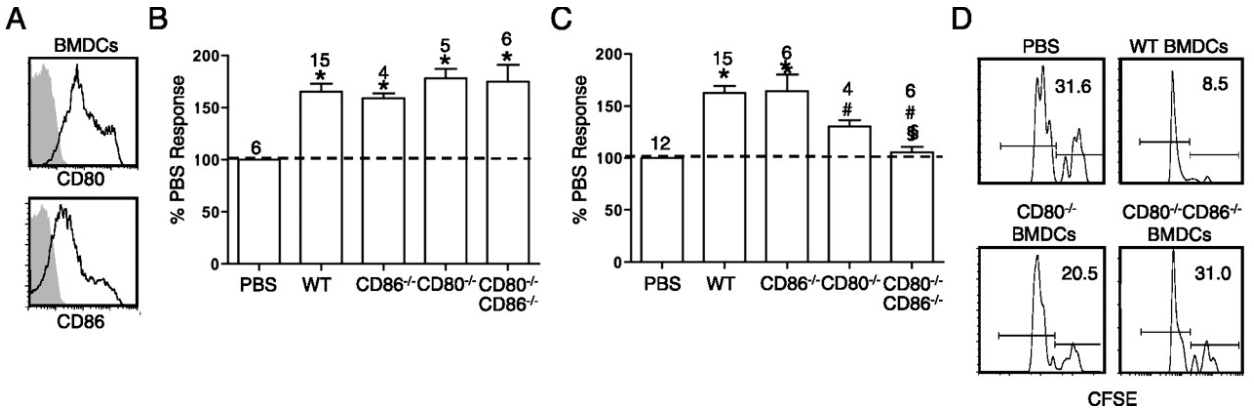

Figure 2. CD80 and CD86 expression on BMDCs is necessary for 2C T cell reactivation but not the delay of 2C T cell tolerance. (A) Day 7 LPS activated BMDCs were stained with anti-CD11c, CD80 or CD86 antibodies (black line) or isotype control (filled grey line). CD80 and CD86 expression histograms are gated on $CD11c^+$ cells. (B and C) Mice were treated and cells analyzed as in Figure 1B with prostate tissues injected with PBS, wild type (WT), $CD80^{-/-}$, $CD86^{-/-}$, or $CD80^{-/-}CD86^{-/-}$ BMDCs on either (B) day 7 or (C) or day 30 after initial 2C cell transfer and infection. Percentages (mean ±standard deviation) of $IFN\gamma^+$ 2C cells from at least three independent experiments are normalized to PBS control. Number of mice for each treatment are indicated. * $p<0.05$ comparing DC versus PBS injection, # $p<0.05$ comparing WT versus knockout DCs, § $p<0.05$ comparing $CD80^{-/-}CD86^{-/-}$ DCs versus $CD80^{-/-}$ DCs. (D) Thirty days post 2C cell transfer and infection, TRP-SIY mice were injected intraprostatically with PBS, or SIY-loaded WT, $CD80^{-/-}$, $CD80^{-/-}/CD86^{-/-}$ BMDC. On day 36, mice were injected retroorbitally with a 1:1 mixture of SIY-pulsed ($CFSE^{Hi}$) and unpulsed ($CFSE^{Lo}$) activated T cells ($Thy1.1^+$). The following day, the proportions of $CFSE^{Hi}$ vs $CFSE^{Lo}$ target cells were determined by flow cytometry. CFSE histograms are shown for live $Thy1.1^+$ cells. Numbers indicate percentage of $CFSE^+$ cells. Representative data from one of the two experiments are shown.

CD86 and CD80 do not affect BMDCs' ability to delay 2C T cell tolerance, indicating other costimulatory molecules may potentiate these effects. TNF costimulatory molecules, such as 4-1BBL and CD70, promote T cell activation during initial priming, and may be important for 2C T cell function during initial infiltration within the prostate tissue (Watts, 2005). We used anti-CD70 and anti-4-1BBL antibodies to define the contribution of CD70 and 4-1BB in DC-mediated delay of tolerance induction. To exclude possible Fc receptor (FcR)-mediated effect on the DCs, we generated $F(ab')_2$ fragment of each antibody lacking the Fc portion of the molecule but still retaining binding activity as assessed by the ability to compete fluorescently labeled full length antibody for cell surface binding (Figure 3*B*). As a control, we used $F(ab')_2$ of the antibody cocktail against FcRs CD16 and CD32. SIY-loaded BMDCs were incubated with each antibody fragment and then injected into prostate tumor tissue of TRP-SIY mice 7 days after 2C T cell transfer and WSN-SIY infection. FcR-blocking antibodies did not diminish the ability of BMDCs to stimulate prolonged IFN-γ expression by infiltrating 2C T cells (Figure 3*C*). Blocking the interaction between 4-1BB on 2C T cells and 4-

1BBL on BMDCs did not impair DCs' ability to extend the IFN-γ expression by infiltrating 2C T cells. However, blockade of CD70 on BMDCs significantly reduced their ability to stimulate prolonged IFN-γ expression by infiltrating 2C T cells in the prostate (Figure 3*C*). These results show that CD70/CD27 interaction is required for DC-mediated delay of 2C T cell tolerance induction in the prostate tumor tissue.

As 4-1BBL and CD70 have been shown to enhance recall responses and reactivate previously tolerized T cells (Keller et al, 2008; Bertram et al, 2002), we examined the effect of 4-1BBL and CD70 on reactivation of already tolerized 2C T cells. We injected antibody-treated, SIY-loaded BMDCs into the prostate of TRP-SIY mice 30 days after 2C T cell transfer and WSN-SIY infection. Blockade of either CD70 or 4-1BBL did not significantly reduce the fractions of persisting 2C T cells that were induced to express IFN-γ (Figure 3*D*), indicating that CD70 and 4-1BBL are not required for reactivation of tolerized 2C T cells in the prostate tumor tissue.

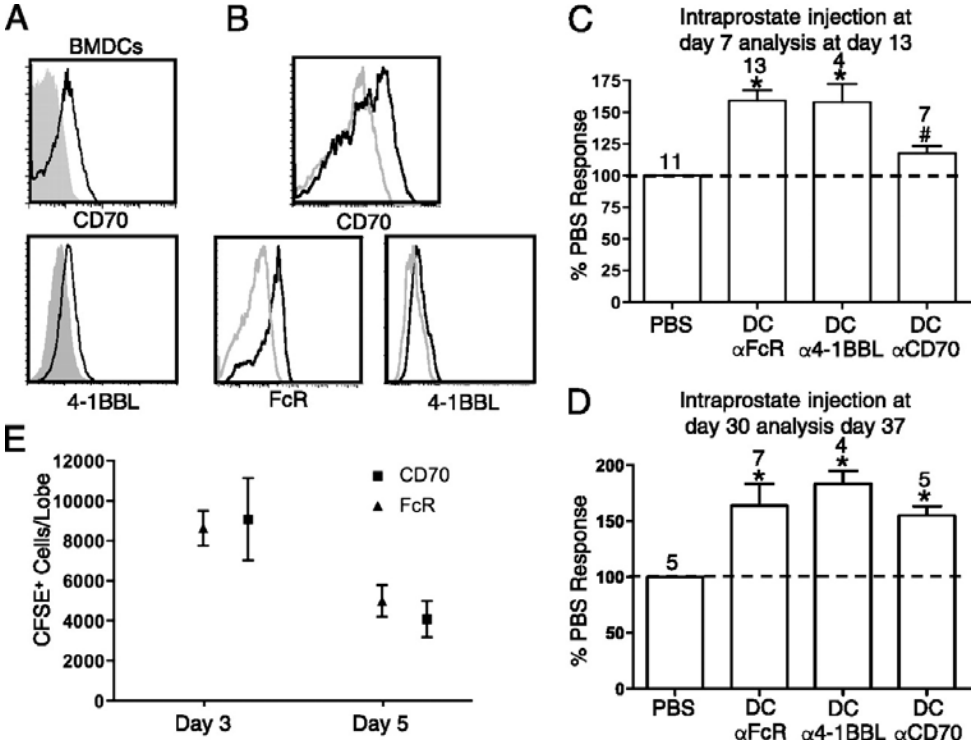

Figure 3. CD70 is required for DC-mediate delay in 2C T cell tolerance. (A) Day 7 LPS activated BMDCs were stained for CD11c plus CD70, 4-1BBL (black line) or isotype control (filled grey line). Histograms are gated on $CD11c^+$ cells. (B) $F(ab')_2$ fragments are confirmed to maintain their antigen binding capacity using a competition assay. BMDCs were incubated with 10 mg/mL of fluorescently labeled full length antibody in the presence of the same amount of either $F(ab')_2$ of interest or control anti-FcR $F(ab')_2$ fragment. The cells were then stained with anti-CD11c and analyzed by flow cytometry. Center histogram shows binding of fluorescently labeled anti-CD70 to BMDCs in the presence of either anti-CD70 $F(ab')_2$ (grey) or control anti-FcR $F(ab')_2$ (black). Left histogram shows binding of fluorescently labeled anti-CD16/CD32 to BMDCs in the presence of either anti-FcR $F(ab')_2$ (grey) or control anti-CD70 $F(ab')_2$ (black). Right histogram shows binding of fluorescently labeled anti-4-1BBL to BMDCs in the presence of either anti-4-1BBL $F(ab')_2$ (grey) or control anti-FcR $F(ab')_2$ (black). Histograms are gated on $CD11c^+$cells.

(C) Experiments were conducted as in Figure 1B with SIY pulsed BMDCs incubated with anti-FcR, CD70, or 4-1BBL $F(ab')_2$ fragments. Shown are percentages (mean ± standard deviation) of $IFN\gamma^+$ 2C cells from three independent experiments normalized to PBS control. Number of mice for each treatment are indicated. (D) As in C, except BMDCs were injected on day 30 post T cell transfer and analysis was carried out on day 37. Shown are percentages (mean ± standard deviation) of $IFN\gamma^+$ 2C cells from three independent experiments normalized to PBS control. Number of mice for each treatment are indicated. * $p<0.05$ comparing DC versus PBS injection, # $p<0.05$ comparing BMDCs treated with anti-CD70 $F(ab')_2$ versus anti-FcR $F(ab')_2$. (E) Day 7 LPS matured BMDCs were labeled with CFSE and incubated with $F(ab')_2$ fragments specific for FcR or CD70. DCs ($10x10^3$/mouse) were surgically injected into one of the dorsal prostate lobes. Three and five days later mice were sacrificed and $CSFE^+$ DCs in each of the prostate tissues were assessed by flow cytometry. Shown are the average numbers of DCs (± standard deviation) from three prostates per group, per time point.

These findings reveal dynamic requirements for costimulatory signals to overcome tumor induced tolerance and have significant implications for developing more effective cancer immunotherapies, including the use of nanoparticle-modified T cells. For example, incorporation of CD70 into the nanoparticle may overcome the tumor induced tolerance of infiltrating T cells and incorporation of CD80/CD86 into the nanoparticle may promote reactivation of infiltrating T cells in the tumor tissue so as to achieve maximal anti-tumor effect. This work has been published in the Journal of Immunology (Bak et al, 2011).

In study associated with Task 3.2, we investigated how prostate cancer cells escape immune-mediated elimination. Tolerization of tumor-infiltrating T cells in the tumor microenvironment is one mechanism that negatively impacts on ACT. Another mechanism that negatively impacts on ACT is the selection and outgrowth of antigen-negative tumor cells. The TRP-SIY system offers a unique opportunity to investigate the second mechanism as antigen-bearing tumor cells express β-galactosidase (β-gal) and the antigen-specific CD8 2C T cells can be identified by Thy1.1 expression (Bai et al, 2008). By determining the relative localization of 2C T cells and β-gal-expressing tumor cells, we show that over time tumor-infiltrating (2C) T cells gradually lose contact with antigen (SIY)-expressing tumor cells in the prostate tissue (Bak et al, submitted).

To determine whether the decrease in T cell/antigen contact within the prostate tissue was due to loss of antigen expression over time, we harvested prostate tissues from age-matched TRP-SIY mice with (treated) or without (untreated) 2C T cell transfer/infection, stained tissue sections for β-gal and quantified the percentage of β-gal staining as a function of total prostate glandular area. TRP-SIY prostates normally contain large areas of epithelia that stained positive for β-gal (Figure 4A, left). Eleven days after 2C T cell treatment, the percentage of β-gal positive areas did not change

significantly (Figure 4A and 4B). However, by 35 and 50 dpt the level of antigen expression was reduced significantly. The loss of SIY-expressing cells was antigen specific as transfer of OT-1 T cells that recognize SIINFEKL (SIIN) epitope and infection with WSN virus that expresses the SIIN epitope (WSN-SIIN) did not induce the loss of β-gal-expressing cells within the prostates of TRP-SIY mice (Figure 4B).

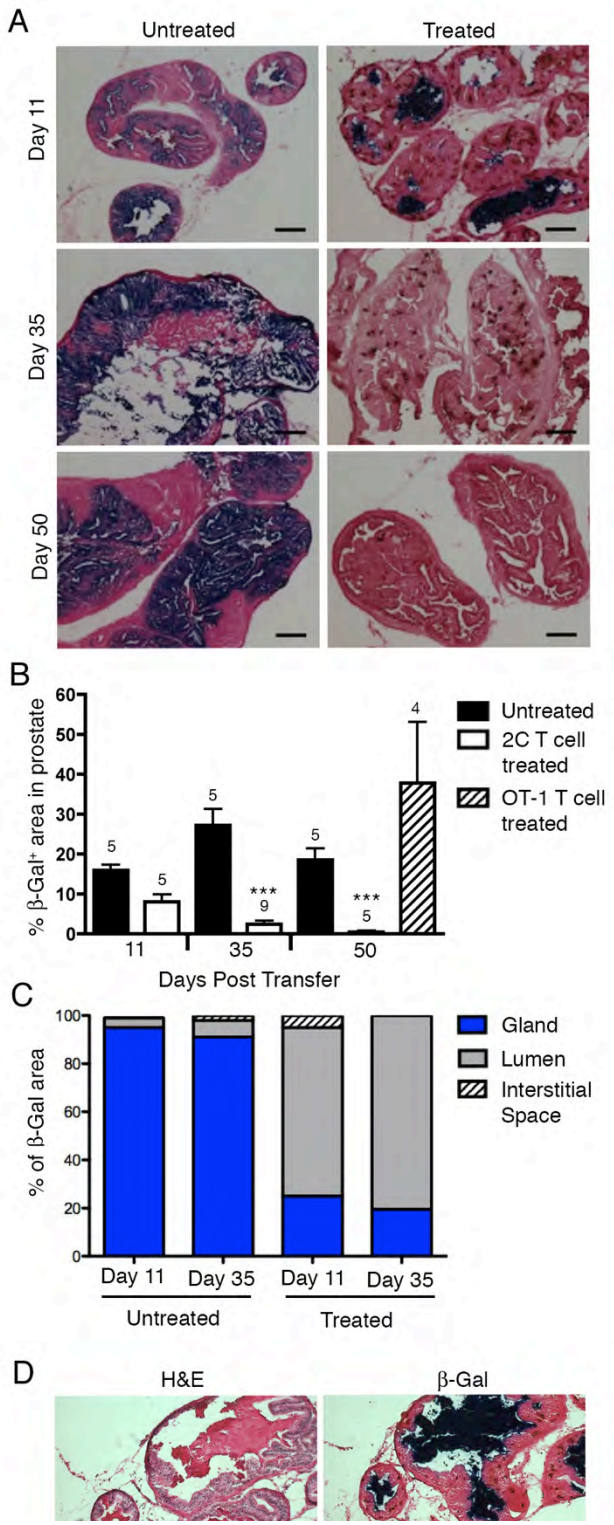

We noticed the spatial distribution of X-gal staining was markedly different between untreated and 2C T cell-treated mice 11 dpt. In untreated mice, β-gal staining was spread throughout the prostate tissue (Figure 4A, top) and over 90% of staining was found in glandular epithelia (Figure 4C). In contrast, in the treated mice ~80% β-gal staining was found in the lumen of prostate glands. To determine whether the luminal β-gal positive areas contained viable cells, we compared consecutive sections of tissue stained with either hematoxylin and eosin (H&E) or X-gal. Luminal areas that stained positive for β-gal after T cell treatment were composed of hematoxylin (nuclear stain) negative and eosin positive (cytoskeleton) cellular debris (Figure 4D). Furthermore, β-gal stains were also detected in the urethra of treated mice (data not shown). These data suggests that the loss of β-gal-expressing tumor cells are likely due to elimination by infiltrating antigen-specific 2C T cells and the mass of dead tumor cells are cleared through the luminal space.

Figure 4. Antigen positive cells are lost from 2C T cell-treated TRP-SIY prostates. Prostate sections from age-matched untreated and treated mice were stained for β-gal, Thy1.1 and eosin and both the β-gal

and Thy1.1-stained areas were quantified. A. Representative images of staining for β-gal (blue) and Thy1.1 (brown) counterstained with eosin (red) of untreated mice and treated mice 11, 35 and 50 dpt. B. Percentages (mean ± SD) of β-gal$^+$ areas in the prostate section of untreated (black) and treated (open) mice at the indicated dpt. Some mice were transferred with OT-1 T cells and infected with WSN-SIIN virus and the percentage of β-gal$^+$ area was quantified 50 dpt (dashed bar). The numbers of mice in each group are indicated. C. β-gal staining was classified as localizing to the gland (blue), lumen (grey) or interstitial space (dash) of the prostate sections from the same group of mice treated in B and expressed as an average percentage of total β-gal staining. D. Representative β-gal (left) ad H&E (left) staining of consecutive prostate sections from a mouse 11 dpt. Scale bars in both A and D, 100μm. ***p value of < 0.001 as compared to untreated group. n.s., not significant.

We next determined whether reduction in antigen expressing prostate cells in treated mice affected tumor progression. To assess tumor progression, H&E stained prostate tissues from 2C treated and untreated mice were blinded and graded for tumor stage (Figure 5A). At 11 dpt the average tumor grade was the same (1.4) in both treated and age-matched control mice (Figure 5A). At 35 dpt the average tumor grade in treated and age matched controls was 2.2 and 2.5, respectively. At 50 dpt the average grade was 3.8 for treated mice versus 2.8 for untreated mice. These data suggest that despite clearance of SIY-expressing cells in the TRP-SIY prostates, tumors continue to grow.

TRP-SIY mice were constructed by introducing β-gal-SIY fusion transgene onto the TRAMP mice, which carry the SV40 large T antigen (Tag) transgene (Bai et al, 2008). Although both transgenes were driven by the same prostate-specific promoter, the two transgenes were introduced into the mouse genome independently. It is possible that activated 2C T cells eliminated SIY-expressing tumors while those that do not express the SIY antigen grow out after T cell treatment. To test this possibility, we stained untreated TRP-SIY prostate sections for both β-gal and Tag. Although most β-gal and Tag staining overlapped, significant fraction of prostate area was stained positive for Tag but negative for β-gal (Figure 5B). Furthermore, to assess the expression of the Tag after 2C T cell treatment we stained treated and untreated prostate sections for Tag (Figure 5C). At all three time points (11, 35 and 50 dpt), the 2C T cell treatment did not affect the percentage of prostate tissue that stained positive for Tag (Figure 5D). However, the percentage of Tag-positive area increased over time following 2C treatment, correlating with tumor progression. Taken together, these data suggest that although 2C T cell treatment is effective in eliminating SIY-positive tumor cells, the SIY-negative tumor cells continue to grow.

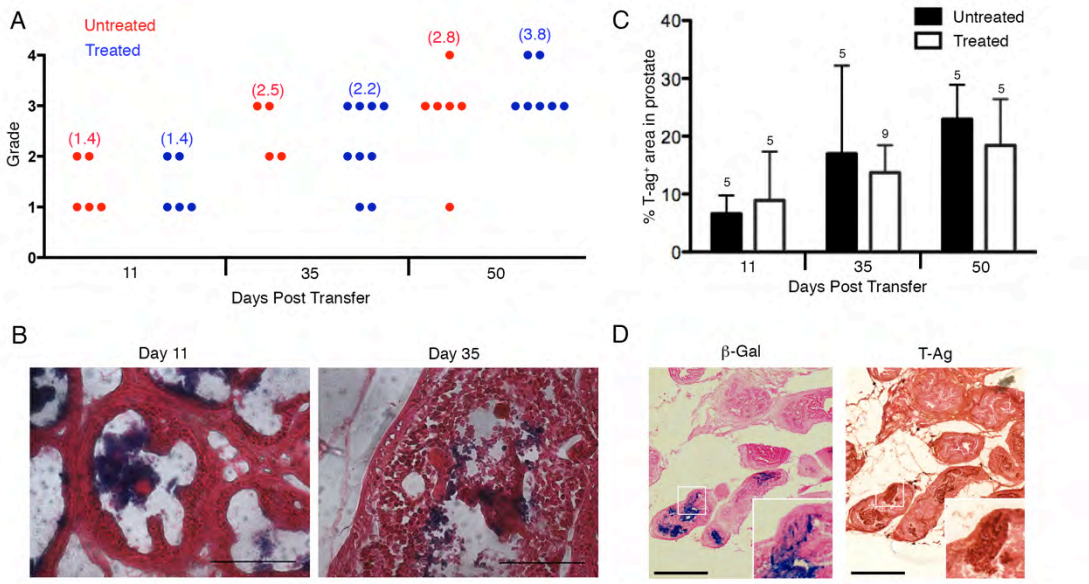

Figure 5. 2C T cell treatment does not affect tumor progression. A. Mice were treated as in Figure 4, prostate sections from both 2C T cell treated and age matched untreated mice were stained with H&E and graded (0, normal tissue; 1, proliferation with no invasion; 2, early invasion; 3, clear-cut invasion; 4, total replacement of organ). Shown are tumor grade at 11, 35, and 50 dpt. Each symbol represents one mouse. The numbers in parentheses indicate the average of tumor grade at each time point. B. Prostate sections from untreated TRP-SIY mice were stained for β-gal (blue), Tag (brown) and eosin (red). Representative images are shown for prostate sections from mice at 16 weeks of age. C and D. Mice were treated as in Figure 2, prostate sections from both 2C T cell treated and age matched untreated mice were stained for Tag (dark brown) and eosin (red). Shown are representative Tag staining of prostate sections from 2C treated mice at 11, 35 and 50 dpt and age-matched untreated mice (C). Percentages (mean ± SD) of Tag^+ areas in the prostate section of untreated and 2C treated mice at the indicated dpt (D). Scale bars in B and C: 100μm.

Together, these results show that CD8 T cells are effective in eliminating antigen-bearing prostate tumor cells but they also select for the outgrowth of antigen-negative tumor cells. These findings provide insights into the requirements for an effective cancer immunotherapy: not only inducing potent immune responses but also avoiding selection and outgrowth of antigen-negative tumor cells. This work has been submitted for publication.

In associated with Aim 3, we have been developing live mouse imaging to monitor tumor size in the prostate. To study *in vivo* antitumor responses, it is necessary to monitor tumor size in live mice over time by live mouse imaging. Current imaging of prostate tumors in mice rely on genetically manipulated cell lines or imprecise quantification of autochthonous tumor growth. Introduction of fluorescent/luminescent

proteins into pre-existing prostate cell lines and their subsequent surgical implantation does not faithfully mimic the natural progression of autochthonous prostate tumor in situ. Analysis of the existing autochthonous prostate tumor mouse models requires MRI, which is costly and technically difficult, and *ex vivo* weight analysis of prostate tissue, which is not compatible with continuous monitoring of tumor growth.

To improve upon these systems, we have developed an inducible prostate cancer model in mice. In our new system (Figure 6), tumor formation is initiated in double transgenic $PTEN^{fl/fl}$ and $p53^{fl/fl}$ mice through injection of lentivirus expressing Cre recombinase into the prostate. To introduce T cell epitopes, the lentiviral vector also expresses the CD8 epitopes SIYRYYGL (SIY) and SIINFEKL (OVA_{257-64}), and the CD4 epitope ISQAVHAAHAEINEAGR ($OVA_{323-339}$). Control virus contains Cre-recombinase but lack model antigens. In addition, the lentiviral vectors express luciferase so that tumor growth can be imaged in live mice. In this system, injection of lentivirus into $PTEN^{fl/fl}/p53^{fl/fl}$ mice induces tumors of prostate origin. These tumors exhibit an aggressive phenotype characterized by invasion into the surrounding genitourinary tract tissue. Furthermore, imaging of luciferase signal from the prostates of these mice is feasible (Figure 7). We have assessed tumor development longitudinally from individual mice by quantitation of the luciferase signal. The increase in luciferase signal from the prostate coincides with the presence of aggressive prostate tumors. We are comparing the effect of tumor immunogenicity on prostate tumor development, through the use of vectors expressing or lacking the CD8 and CD4 epitopes described above. This model will provide an important tool for determining the effect of tumor specific nanoparticle-modified T cells on long term tumor growth.

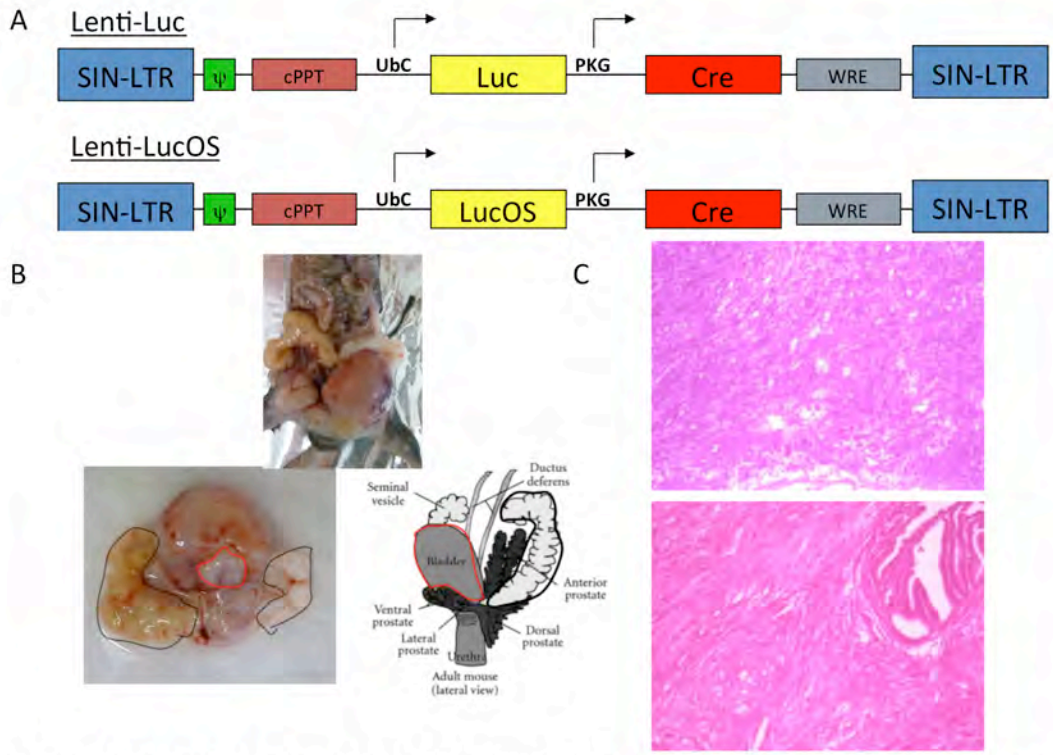

Figure 6. A. Schematic diagrams of the antigenic and non-antigenic lentiviral vectors. B. Representative tumor mass generated from lentivirus injection into PTEN^{flox}p53^{flox} mice. C. Representative H&E section from tumor mass, demonstrating the undifferentiated, aggressive phenotype.

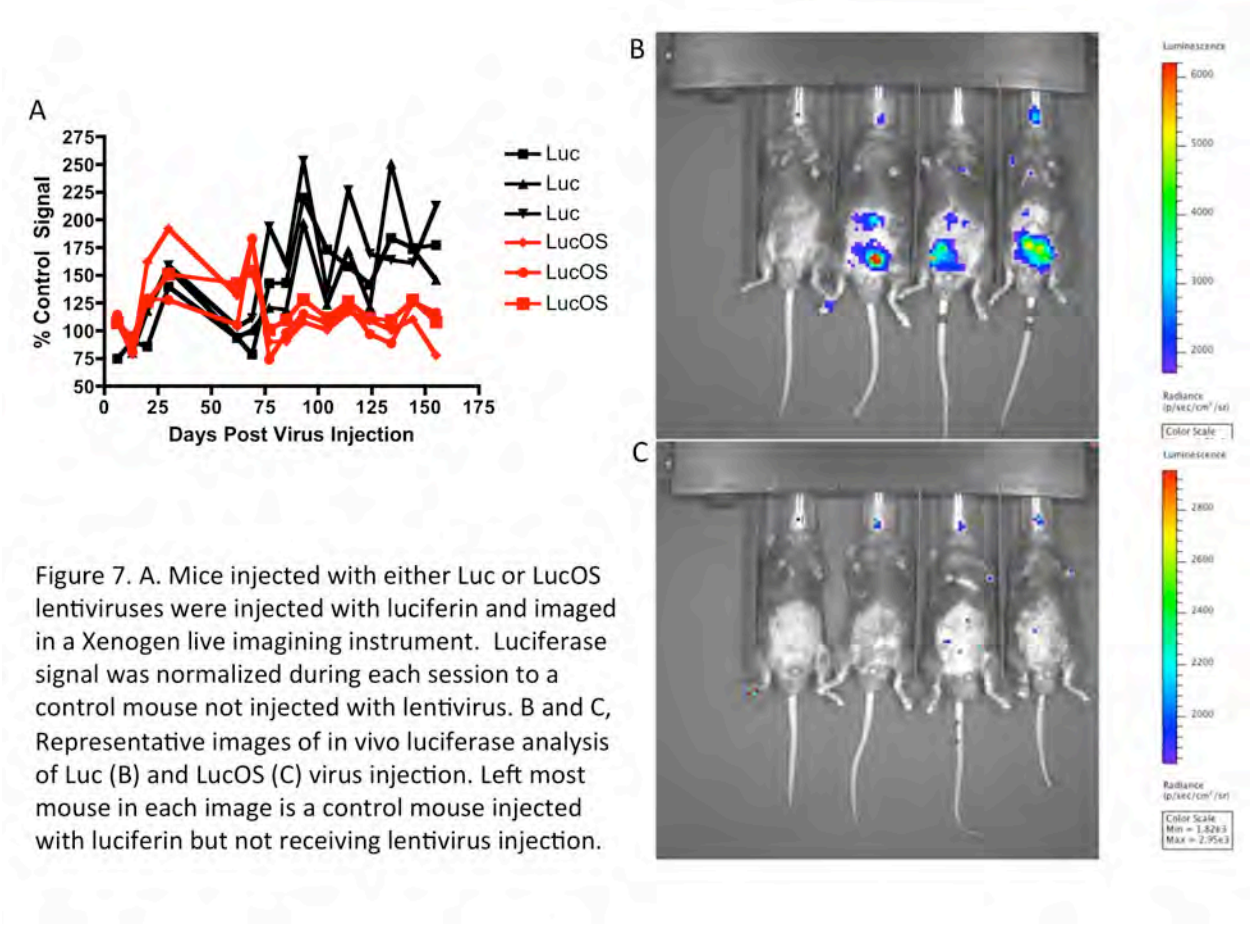

Figure 7. A. Mice injected with either Luc or LucOS lentiviruses were injected with luciferin and imaged in a Xenogen live imagining instrument. Luciferase signal was normalized during each session to a control mouse not injected with lentivirus. B and C, Representative images of in vivo luciferase analysis of Luc (B) and LucOS (C) virus injection. Left most mouse in each image is a control mouse injected with luciferin but not receiving lentivirus injection.

Development of the new model addresses the deficiencies in current prostate tumor models through the ability to: 1) track tumor growth by quantitative *in vivo* imaging, 2) assess endogenous tumor specific T cells using defined antigens, 3) delete specified genes known to effect prostate tumor growth in humans, and 4) dissect the effect of the endogenous immune response to tumors. Development of this new model system will facilitate the *in vivo* analysis of anti-tumor responses by nanoparticle-modified T cells.

Key Research Accomplishment

- Define the role of CD70 and CD80/CD86 in dendritic cell-mediated activation of tumor tolerized CD8 T cells.
- Discover the effect of CD8 T cell responses in selecting for antigen-negative tumor cells in the prostate.
- Develop a better prostate model for monitoring T cell responses to prostate cancer in mice.

Reportable Outcomes

Publications

- Bak SP, Barnkob MS, Bai A, Higham EM, Wittrup KD, Chen J. (2012) Differential requirement for CD70 and CD80/CD86 in dendritic cell-mediated activation of tumor tolerized CD8 T cells. J. Immunol. 189:1708-16. PMID: 22798683.
- Stephan MT, Stephan SB, Bak P, Chen J, Irvine DJ (2012) Synapse-directed delivery of immunomodulators using T-cell-conjugated nanoparticles. Biomaterials, 33:5776.
- Bak SP, Barnkob MS, Wittrup KD, Chen J. CD8 T cell responses rapidly select for antigen-negative tumor cells in the prostate. Submitted.

Presentations

- May 2011, International Symposium on Immunology, Systems Biology and Translational Medicine (ISM Symposium), Changchun, China
- Dec 2012, Department of Microbiology and Immunology, Dartmouth Medical School, Hanover, NH
- June 2013, Koch Institute for Integrative Cancer Research at MIT 2013 Symposium, Cambridge, MA

Conclusion

To realize the full potential of the adoptive cell therapy (ACT) of cancer, we have to overcome the tolerization of the transferred T cells in the tumor environment. Findings from our studies identify molecular interactions that are important for maintaining T cell function in the tumor environment. Our findings suggest that intervention through these targets could potentially enhance T cell functionality during ACT. Furthermore, elucidation of selection of antigen-negative tumor cells by immune responses sheds light on possible development of tumor resistance to ACT and points out possible approaches to overcome this potential problem in advance. Finally, development of a better model for monitoring T cell responses to prostate cancer would facilitate development of immunotherapy for prostate cancer.

References

Bai, A., E. Higham, H. N. Eisen, K. D. Wittrup, and J. Chen. 2008. Rapid tolerization of virus-activated tumor-specific CD8+ T cells in prostate tumors of TRAMP mice. *Proc Natl Acad Sci U S A* 105:13003.

Bak SP, Barnkob MS, Bai A, Higham EM, Wittrup KD, Chen J. 2012. Differential requirement for CD70 and CD80/CD86 in dendritic cell-mediated activation of tumor tolerized CD8 T cells. J. Immunol. 189:1708.

Bak SP, Barnkob MS, Wittrup KD, Chen J. CD8 T cell responses rapidly select for antigen-negative tumor cells in the prostate. Submitted.

Bertram, E. M., P. Lau, and T. H. Watts. 2002. Temporal segregation of 4-1BB versus CD28-mediated costimulation: 4-1BB ligand influences T cell numbers late in the primary response and regulates the size of the T cell memory response following influenza infection. *J Immunol* 168:3777-3785.

Fife, B. T., and J. A. Bluestone. 2008. Control of peripheral T-cell tolerance and autoimmunity via the CTLA-4 and PD-1 pathways. *Immunol Rev* 224:166-182.

Fuse, S., W. Zhang, and E. J. Usherwood. 2008. Control of memory CD8+ T cell differentiation by CD80/CD86-CD28 costimulation and restoration by IL-2 during the recall response. *J Immunol* 180:1148-1157.

Habib-Agahi, M., T. T. Phan, and P. F. Searle. 2007. Co-stimulation with 4-1BB ligand allows extended T-cell proliferation, synergizes with CD80/CD86 and can reactivate anergic T cells. *Int Immunol* 19:1383-1394.

Higham, E. M., C. H. Shen, K. D. Wittrup, and J. Chen. 2010. Cutting edge: delay and reversal of T cell tolerance by intratumoral injection of antigen-loaded dendritic cells in an autochthonous tumor model. *J Immunol* 184:5954.

June, CH, (2007) Principles of adoptive T cell cancer therapy. *J Clin Invest* 117:1204.

Keller, A. M., A. Schildknecht, Y. Xiao, M. van den Broek, and J. Borst. 2008. Expression of costimulatory ligand CD70 on steady-state dendritic cells breaks CD8+ T cell tolerance and permits effective immunity. *Immunity* 29:934-946.

Rosenberg, SA, Restifo, NP, Yang, JC, Morgan, RA, and Dudley, ME, (2008) Adoptive cell transfer: a clinical path to effective cancer immunotherapy. *Nat Rev Cancer* 8:299.

Sharpe, A. H. 2009. Mechanisms of costimulation. *Immunol Rev* 229:5-11.

Watts, T. H. 2005. TNF/TNFR family members in costimulation of T cell responses. *Annu Rev Immunol* 23:23-68.

Appendices

Bak SP, Barnkob MS, Bai A, Higham EM, Wittrup KD, Chen J. 2012. Differential requirement for CD70 and CD80/CD86 in dendritic cell-mediated activation of tumor tolerized CD8 T cells. J. Immunol. 189:1708.

Bak SP, Barnkob MS, Wittrup KD, Chen J. CD8 T cell responses rapidly select for antigen-negative tumor cells in the prostate. Submitted.

THE JOURNAL OF IMMUNOLOGY

Differential Requirement for CD70 and CD80/CD86 in Dendritic Cell-Mediated Activation of Tumor-Tolerized CD8 T Cells

S. Peter Bak, Mike Stein Barnkob, Ailin Bai, Eileen M. Higham, K. Dane Wittrup and Jianzhu Chen

J Immunol 2012; 189:1708-1716; Prepublished online 13 July 2012;
doi: 10.4049/jimmunol.1201271
http://www.jimmunol.org/content/189/4/1708

The Journal of Immunology is published twice each month by
The American Association of Immunologists, Inc.,
9650 Rockville Pike, Bethesda, MD 20814-3994.

Print ISSN: 0022-1767 Online ISSN: 1550-6606.

Differential Requirement for CD70 and CD80/CD86 in Dendritic Cell-Mediated Activation of Tumor-Tolerized CD8 T Cells

S. Peter Bak,*,† Mike Stein Barnkob,* Ailin Bai,*,†,[1] Eileen M. Higham,*,‡,[2] K. Dane Wittrup,*,‡,§ and Jianzhu Chen*,†

A major obstacle to efficacious T cell-based cancer immunotherapy is the tolerizing-tumor microenvironment that rapidly inactivates tumor-infiltrating lymphocytes. In an autochthonous model of prostate cancer, we have previously shown that intratumoral injection of Ag-loaded dendritic cells (DCs) delays T cell tolerance induction as well as refunctionalizes already tolerized T cells in the tumor tissue. In this study, we have defined molecular interactions that mediate the effects of DCs. We show that pretreating Ag-loaded DCs with anti-CD70 Ab abolishes the ability of DCs to delay tumor-mediated T cell tolerance induction, whereas interfering with 4-1BBL, CD80, CD86, or both CD80 and CD86 had no significant effect. In contrast, $CD80^{-/-}$ or $CD80^{-/-}CD86^{-/-}$ DCs failed to reactivate already tolerized T cells in the tumor tissue, whereas interfering with CD70 and 4-1BBL had no effect. Furthermore, despite a high level of programmed death 1 expression by tumor-infiltrating T cells and programmed death ligand 1 expression in the prostate, disrupting programmed death 1/programmed death ligand 1 interaction did not enhance T cell function in this model. These findings reveal dynamic requirements for costimulatory signals to overcome tumor-induced tolerance and have significant implications for developing more effective cancer immunotherapies. *The Journal of Immunology*, **2012, 189: 1708–1716.**

A major focus of cancer immunotherapy has been stimulating patients' $CD8^+$ cytolytic T cells to kill tumor cells. In one treatment modality, tumor-infiltrating leukocytes (TILs) are isolated from the patient, activated ex vivo, and infused back into the same patient. Such adoptive cell therapy (ACT) has shown clinical benefit in treating melanoma (1). In another treatment modality, dendritic cell (DC)-based vaccines are used to stimulate the patients' endogenous anti-tumor immune response, and recently has been approved for treating prostate cancer (2). Despite these successes, a major hurdle to widespread use of these and other treatments using $CD8^+$ T cells is the tolerizing environment within the tumor tissue (1), which rapidly inactivates TILs and renders the therapies ineffective.

T cell activation and function are regulated by both costimulatory and inhibitory signals. In concert with peptide MHC (pMHC) and TCR signaling, additional receptors on T cells promote or negate expansion, differentiation, and survival (3). Programmed death 1 (PD-1) expressed on activated T cells inhibits T cell function upon engagement with its ligand, programmed death ligand 1 (PD-L1). PD-L1 is expressed on tumor and/or tumor-associated stroma, and sites of immune privilege, and is considered a promising candidate for checkpoint blockade in tumor immunotherapy (4). Indeed, blockade of PD-L1, along with adoptive transfer of tumor-specific T cells, delays tumor growth in preclinical melanoma models (5). Among costimulatory molecules, engagement of CD28 on T cells with CD80 and CD86 on APCs promotes activation of both naive and memory T cells (3). Specific to anti-tumor responses, enforced expression of CD80 and/or CD86 on tumor cells stimulates their destruction by the immune system (6), a strategy of cancer immunotherapy that has been tested in clinical trials (7). The TNF family contains a diverse array of molecules critical for positively regulating T cell function, including the CD27/CD70 and 4-1BB/4-1BBL receptor ligand pairs, expressed on T cells and APCs, respectively (8). Overexpression of CD70 in transgenic mice enhances priming of T cells, leading to rejection of EL-4 thymomas that express the nucleoprotein model Ag (9). Similarly, in vivo stimulation of clonotypic T cells with an anti–4-1BB Ab promotes T cell rejection of established murine plasmacytoma tumors (10).

In our study of $CD8^+$ T cell/tumor cell interaction, we have developed an autochthonous Transgenic Adenocarcinoma of the Mouse Prostate (TRAMP) mice expressing SIY (TRP-SIY) prostate cancer model, based on TRAMP mice, in which tumor cells express a nominal MHC class I epitope (SIYRYYGL or SIY) recognized by the 2C clonotypic TCR (11). Adoptive transfer of naive $CD8^+$ 2C T cells into TRP-SIY mice, followed by infection with influenza virus expressing the SIY epitope, leads to activation and differentiation of transferred T cells into potent effector cells.

*Koch Institute for Integrative Cancer Research, Massachusetts Institute of Technology, Cambridge, MA 02139; †Department of Biology, Massachusetts Institute of Technology, Cambridge, MA 02139; ‡Department of Biological Engineering, Massachusetts Institute of Technology, Cambridge, MA 02139; and §Department of Chemical Engineering, Massachusetts Institute of Technology, Cambridge, MA 02139

[1]Current address: AVEO Pharmaceuticals, Cambridge, MA.

[2]Current address: MedImmune, Gaithersburg, MD.

Received for publication May 8, 2012. Accepted for publication June 17, 2012.

This work is supported in part by a Postdoctoral Fellowship (12109-PF-11-025-01-LIB) from the American Cancer Society (to S.P.B.), the Margaret A. Cunningham Immune Mechanisms in Cancer Research Fellowship (to S.P.B.) from the John D. Proctor Foundation, and a Prostate Cancer Research Program grant from the United States Army Medical Research and Materiel Command (to J.C.).

Address correspondence and reprint requests to Prof. Jianzhu Chen, Koch Institute for Integrative Cancer Research, Massachusetts Institute of Technology, Cambridge, MA 02139. E-mail address: jchen@mit.edu

The online version of this article contains supplemental material.

Abbreviations used in this article: ACT, adoptive cell therapy; BMDC, bone marrow-derived dendritic cell; DC, dendritic cell; PD-1, programmed death 1; PD-L1, programmed death ligand 1; pMHC, peptide MHC; TIL, tumor-infiltrating lymphocyte; TRAMP, Transgenic Adenocarcinoma of the Mouse Prostate; TRP-SIY, TRAMP mice expressing SIY; WSN-SIY, WSN influenza A virus strain expressing SIY.

www.jimmunol.org/cgi/doi/10.4049/jimmunol.1201271

As in human patients, effector T cells infiltrate the prostate tumor tissue and rapidly become inactivated (tolerized). The tolerized 2C T cells persist in the prostate tumor tissue (12), expressing high levels of PD-1, analogous to TILs in patients. Importantly, we have found that Ag-loaded bone marrow-derived DCs (BMDCs), when injected intraprostatically, delay the rapid tolerance induction of effector 2C T cells as they initially infiltrate the tumor tissue (13). In addition, when Ag-loaded BMDCs are injected after initial tolerance induction, they refunctionalize the persisting tolerized 2C T cells in the tumor tissue. These previous studies set the stage for defining molecular interactions that are required for prostate tumor-mediated T cell tolerance induction and DC-mediated delay and reactivation of tolerized T cells in the prostate tumor microenvironment.

In this study, we have evaluated the role of PD-1/PD-L1 interaction in T cell tolerance induction in prostate tumor tissue and the role of CD80, CD86, 4-1BBL, and CD70 in DC-mediated delay of T cell tolerance induction and refunctionalization of tolerized T cells in prostate tumor tissue. Our results show that despite the high levels of PD-1 expression by prostate-infiltrating T cells and PD-L1 expression in the prostate, blocking PD-1/PD-L1 interaction has no effect on T cell tolerance induction in prostate tumor tissue. Although CD70 is required for DC-mediated delay of T cell tolerance induction, CD80 and CD86 are necessary for refunctionalizing the tolerized T cells in prostate tumor tissue. These findings show that different costimulatory signals are required to overcome tumor-tolerizing signals during the initial tolerance induction and reactivation of previously tolerized T cells. They also suggest approaches to overcoming the tolerizing tumor environment, to achieve more efficacious cancer immunotherapy by ACT and DC vaccination.

Materials and Methods

Mice, adoptive transfer, and influenza infection

TRP-SIY mice were generated as previously described (11). 2C TCR transgenic mice were maintained on C57BL/6 and RAG1$^{-/-}$ backgrounds (2C/RAG mice). CD86 and CD80/CD86 knockout mice on the C57BL/6 background were from The Jackson Laboratory (Bar Harbor, ME). CD80, PD-L1 knockout, and TRAMP mice were bred in house. Where indicated, mice were retro-orbitally injected with 1.5×10^6 naive 2C cells from 2C/RAG mice and were intranasally infected with 100 PFU WSN influenza A virus strain expressing SIY (WSN-SIY) influenza A virus. All experiments were approved by the Committee on Animal Care at Massachusetts Institute of Technology.

Generation of BMDCs and intraprostatic injection

Bone marrow was collected from the femurs of C57BL/6 mice or indicated knockout mice. Cells were resuspended at 2×10^5 cells per milliliter in RPMI 1640 plus 10% FCS, 50 μM 2-ME, 4 mM L-glutamine, and 100 U/ml–100 μg/ml penicillin–streptomycin supplemented 1:30 with supernatant from J5 cells secreting GM-CSF. Cells were washed and media changed on days 2 and 5, 1 μg/ml LPS was added on day 6, and cells were harvested on day 7. Where indicated, BMDCs were loaded with 1 μg/ml SIY peptide for 1 h at 37°C and/or were labeled for 10 min at 37°C with 5 μM CFSE (Invitrogen) in PBS plus 0.1% BSA on the day of harvest. For blocking experiments, 1×10^6 cell/ml were incubated in 10 μg/ml F(ab′)$_2$ of indicated Abs for 2.5 h on ice, as previously described (14). BMDCs were rinsed and resuspended at 1×10^6 cells per 40 μl PBS for intraprostatic injection (1×10^6 cells per mouse).

Cells and flow cytometry

Single-cell suspensions were prepared from lymphoid tissues by grinding them between frosted glass slides and filtering the suspensions through 70-μm nylon mesh. Prostate tissues were digested with 2 μg/ml collagenase A (Roche) and 170 U/ml DNase I (Sigma-Aldrich, St. Louis, MO) in RPMI 1640 plus 10% FCS for 1 h at 37°C. Digested samples were then ground between frosted glass slides and filtered through 70-μm nylon mesh. Intracellular IFN-γ staining was performed with a BD Cytofix/Cytoperm Kit (BD Biosciences). Recovered cells were restimulated with 1 μg/ml SIY peptide for 4 h at 37°C in the presence of BD GolgiPlug containing brefeldin A. Surface Ags were stained, dead cells were identified using a LIVE/DEAD Fixable Red Dead Cell Stain Kit (Invitrogen), and all cells were fixed and permeabilized. Samples were then stained with a PE-conjugated anti–IFN-γ Ab (BD Pharmingen). Gates were set using a panel of fluorescent minus one controls. Statistical analysis was conducted using a Student *t* test and data were considered significant if $p < 0.05$.

Immunohistochemistry

Prostate glands were excised from mice, flash frozen in OCT compound (Tissue-Tek; Sakura, Torrance, CA), and cryosectioned at 10 μM by the Koch Institute Histology Core Facility. Sections were fixed with acetone and stained with Vectastain Elite ABC Kit (Vector Laboratories, Burlingame, CA). Visualization of PD-L1 staining was carried out with 3,3′-diaminobenzidine substrate (Vector Laboratories) and counterstained with eosin (Sigma-Aldrich). Images were acquisitioned using a Zeiss Axioplan II microscope, with Zeiss 25× (0.8) lenses and a QImaging MicroPublisher 5.0 color camera. Images were captured using Openlab 5.5 (Improvision; PerkinElmer) and analyzed using ImageJ (National Institutes of Health).

Abs and F(ab′)$_2$ production

Fluorescently labeled Anti-Thy1.1 (Clone OX-7), CD27 (LG.3A10), CD11c (N418), CD28 (37.51), PD1 (RMP1-30), 41BB (17B5), OX40 (OX-86), CD30 (CD30.1), and LAG-3 (C9B7W) were from BioLegend; anti-CD86 (P03.1), CD70 (FR70), 4-1BB-L (TKS-1), PD-L1 (MIH5), and Tim3 (8B.2C12) from eBioscience; anti-CD80 (16-10A1), CD44 (IM7), and rat IgG2bκ isotype (clone A95-1) from BD Pharmingen; and biotinylated anti-rat IgG (BA-4001) from Vector Laboratories. 2C TCR was stained using a biotin-conjugated clonotypic 1B2 Ab detected with streptavidin-APC (BioLegend). Stained cells were analyzed using a FACSCalibur or LSR II (BD Biosciences) instrument, and the data were processed using FlowJo software (Tree Star).

F(ab′)$_2$ fragments were generated from purified anti-CD70 (FR70; eBioscience), anti–4-1BBL (TKS-1; eBioscience), anti-FcR (CD16/CD32) (2.4G2; BD Pharmingen) using the Pierce F(ab′)$_2$ Preparation Kit (Thermo Scientific) and concentration determined by absorbance on 280 nm, as recommended. For F(ab′)$_2$ competition experiments, 1×10^6 cells per milliliter were incubated in 10 μg/ml F(ab′)$_2$ fragment and full-length fluorescently labeled Ab, followed by staining with CD11c and analysis by flow cytometry.

In vivo cytotoxicity assay

In vivo cytotoxicity was performed as previously described (13). Briefly, C57BL/6 (Thy1.1$^+$) splenocytes were activated on anti-CD3–coated plates in the presence of 50 U/ml IL-2 for 3 d. Half of the activated splenocytes were then labeled with 20 μM CFSE (CFSE^{Hi}) and pulsed with SIY peptide, and half were labeled with 1 μM (CFSE^{Lo}). CFSE^{Hi} and CFSE^{Lo} cells were mixed 1:1 and retroorbitally injected into mice (20×10^6 cells per mouse). Approximately 24 h later, the ratio of DC CFSE^{Hi} to CFSE^{Lo} cells in various tissues was evaluated by flow cytometry.

Results

PD-1 is expressed on prostate resident T cells and PD-L1 on the prostate stroma

To define the pathways that regulate tolerance of 2C T cells in the TRP-SIY system, we assessed the expression of inhibitory receptors on the surface of 2C T cells. PD-1, Tim3, and LAG-3, individually or in combination, negatively regulate T cell responses in tumor tissues (15, 16). T cells recovered 13 days post transfer, (or ~6 d after initial infiltration into the prostate) expressed high levels of PD-1 (Fig. 1A). Expression of PD-1 was maintained on prostate resident 2C T cells beyond 36 d post transfer into TRP-SIY mice (Fig. 1A). In contrast to PD-1, prostate resident 2C T cells did not express Tim3 or LAG-3 either 13 or 36 d post transfer (Fig. 1B, 1C). PD-L1 expression was detected on both C57BL/6-SIY and TRP-SIY prostate cells by flow cytometry (Fig. 1D) and confirmed by histological staining of prostate tissue sections (Fig. 1E).

Modulating the PD-1/PD-L1 axis does not improve T cell responses in TRP-SIY mice

The expression of PD-1 on 2C T cells and PD-L1 on prostate cells provides the basis for a possible role of PD-1/PD-L1 interaction in

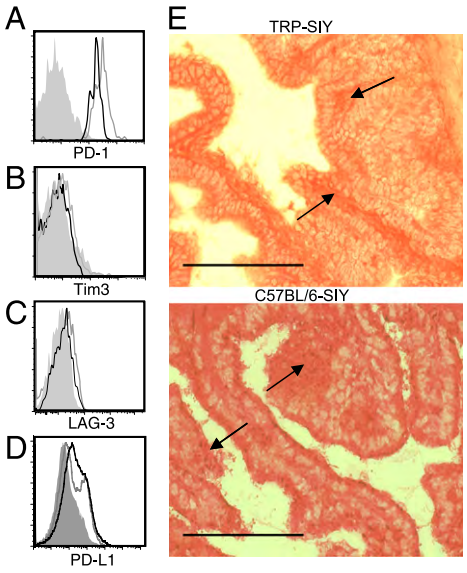

FIGURE 1. PD-1 is expressed on prostate resident T cells and PD-L1 on the prostate stroma. Naive 2C T cells were transferred into TRP-SIY mice, followed by intranasal infection with WSN-SIY virus. Prostates were harvested day 13 and day 36 post transfer, and Thy1.1$^+$2C TCR$^+$ cells were analyzed for PD-1 (**A**), Tim3 (**B**), or LAG-3 (**C**) expression. Histograms show relative levels of cell surface expression on 2C T cells at day 13 (gray) or day 36 (black), compared with isotype control (filled gray line). (**D**) Prostates from TRP-SIY (black) and C57BL/6-SIY (gray) mice were harvested and digested into single-cell suspension and stained with PD-L1 or isotype (filled gray line) and analyzed by flow cytometry. Histograms show relative levels of PD-L1 expression on prostate cells. (**E**) Sectioned prostates of TRP-SIY and C57BL/6-SIY mice were stained for PD-L1, visualized with peroxidase staining (brown), and counterstained with eosin (red). Arrows indicate areas of positive staining. Scale bars, 100 μm.

tolerance induction in the TRP-SIY system. To test this idea, we generated TRP-SIY mice on a PD-L1$^{-/-}$ background. Following adoptive transfer of 2C T cells and intranasal infection with WSN-SIY influenza virus, effector 2C T cells infiltrated the prostate tumor tissue of TRP-SIY PD-L1$^{-/-}$ mice but rapidly lost IFN-γ expression, comparable to 2C T cells in prostates of TRP-SIY mice heterozygous for PD-L1 (Fig. 2A). Thus, PD-L1 is not required for T cell tolerance induction in the prostate tumor tissue of TRP-SIY mice.

Although PD-L1 expression was not directly responsible for tolerance induction, the expression of PD-1 on 2C T cells could affect their subsequent function. Therefore, we tested whether the PD-1/PD-L1 interaction between 2C T cells and BMDCs affects the BMDC-mediated activation of 2C T cells. 2C T cells were transferred into TRP-SIY mice and activated by intranasal WSN-SIY infection. Seven days later, as newly induced effector 2C T cells entered the prostate, SIY-loaded BMDCs from wild-type or PD-L1$^{-/-}$ mice were injected directly into prostate tumor tissue to test whether they delay the tolerance induction (Fig. 2B). 2C T cells were recovered from the prostate an additional 6 d later and analyzed for their ability to express IFN-γ. Intraprostatic injection of SIY-loaded wild-type or PD-L1$^{-/-}$ BMDCs stimulated similar percentages of 2C T cells to express IFN-γ when compared with PBS control (Fig. 2C, 2D). Furthermore, 30 d after initial T cell transfer and infection, when infiltrating 2C T cells were already tolerized, SIY-loaded BMDCs from wild-type or PD-L1$^{-/-}$ mice were injected intraprostatically to assess whether they reactivate the tolerized T cell in situ to a similar extent (Fig. 2B). Intraprostatic injection of SIY-loaded wild-type or PD-L1$^{-/-}$ BMDCs reactivated similar percentages of 2C T cells to express IFN-γ as compared with PBS control (Fig. 2C, 2E). These results were further confirmed using blocking Abs to PD-L1 (Supplemental Fig. 1). To determine whether PD-L1$^{-/-}$ BMDCs affect the number of 2C T cells within the prostate, we analyzed the numbers of 2C T cells recovered from the prostates after BMDC injection 7 or 30 d post transfer (Fig. 2F, 2G). Injection of PD-L1$^{-/-}$ BMDCs did not increase the number of 2C T cells as compared with PBS or wild-type BMDCs at either time point. Taken together, these data suggest that despite expression of PD-1 on 2C T cells and PD-L1 in the prostate tissue, disruption of PD-1/PD-L1 interaction does not enhance DC-mediated delay of tolerance induction or refunctionalization of already tolerized T cells in prostate tumor tissue.

BMDCs act directly on 2C T cells in the TRP-SIY prostate

We assessed the mechanisms by which BMDCs activate 2C T cells within the prostate tissue. To exclude the possibility that injected BMDCs nonspecifically activate 2C T cells in the prostate, we measured IFN-γ expression by endogenous SIY–non-specific CD8$^+$ T cells. Injection of BMDCs either 7 or 30 d after Thy1.1$^+$ 2C T cell transfer did not stimulate IFN-γ production by endogenous Thy1.1$^-$CD8$^+$ T cells (Fig. 3A). To determine whether injection of activated BMDCs affects endogenous prostate-resident DCs, we assessed costimulatory receptor expression by the endogenous CD11c$^+$ population following injection of either PBS or BMDCs. Compared with PBS injection, injection of activated BMDCs into the prostate of TRP-SIY did not alter the expression of CD80, CD86, CD70, or 4-1BBL on endogenous CD11c$^+$ cells from the prostate (Fig. 3B). Furthermore, injection of SIY-loaded BMDCs did not stimulate IL-2 production by 2C T cells either 7 or 30 d after 2C T cell transfer as compared with PBS (Fig. 3C).

In our experimental system, 2C T cells are activated in the periphery by WSN-SIY infection, and CD44$^+$ effector 2C T cells traffic to the prostate (Fig. 3D). We therefore confirmed that the activity of injected BMDCs is dependent on the direct presentation of SIY peptide to 2C T cells. We compared the effect of injecting PBS, SIY peptide alone, or activated BMDCs that had not been pulsed with the SIY peptide on IFN-γ expression by 2C T cells in the prostate. Injection of SIY peptide alone did not significantly stimulate IFN-γ expression by 2C T cells above control PBS injection (Fig. 3E), suggesting that presentation of SIY by endogenous DCs is not a major factor in reactivation of 2C T cells. Injection of activated BMDCs without being loaded with the SIY peptide in vitro stimulated a higher fraction of 2C T cells to produce IFN-γ (Fig. 3E) than did PBS or SIY peptide alone. However, the effect was less than that with SIY-loaded BMDCs (compare with Fig. 2). The observed effect is not likely due to a nonspecific effect of injected BMDCs but is likely due to uptake and presentation of SIY peptide in the prostate of TRP-SIY mice, where the SIY transgene is robustly expressed (11). Taken together, these results suggest that BMDCs activate 2C T cells in the prostate tumor partly by directly engaging 2C T cells through pMHC/TCR interaction.

CD80 and CD86 are required to reactivate tolerized T cells in prostate tumor tissue

Next, we determined cell surface molecules on BMDCs that are required for reactivating 2C T cells, in addition to SIY/MHC. Upregulated upon maturation of DCs, CD80 and CD86 provide an important stimulus in the context of the TCR/peptide MHC-1 engagement (3). Specific to prostate cancer, provision of antagonistic CD80 or CD86 Abs abrogates the immunosuppressive environment and reduces tumor growth (17). BMDCs exhibit robust

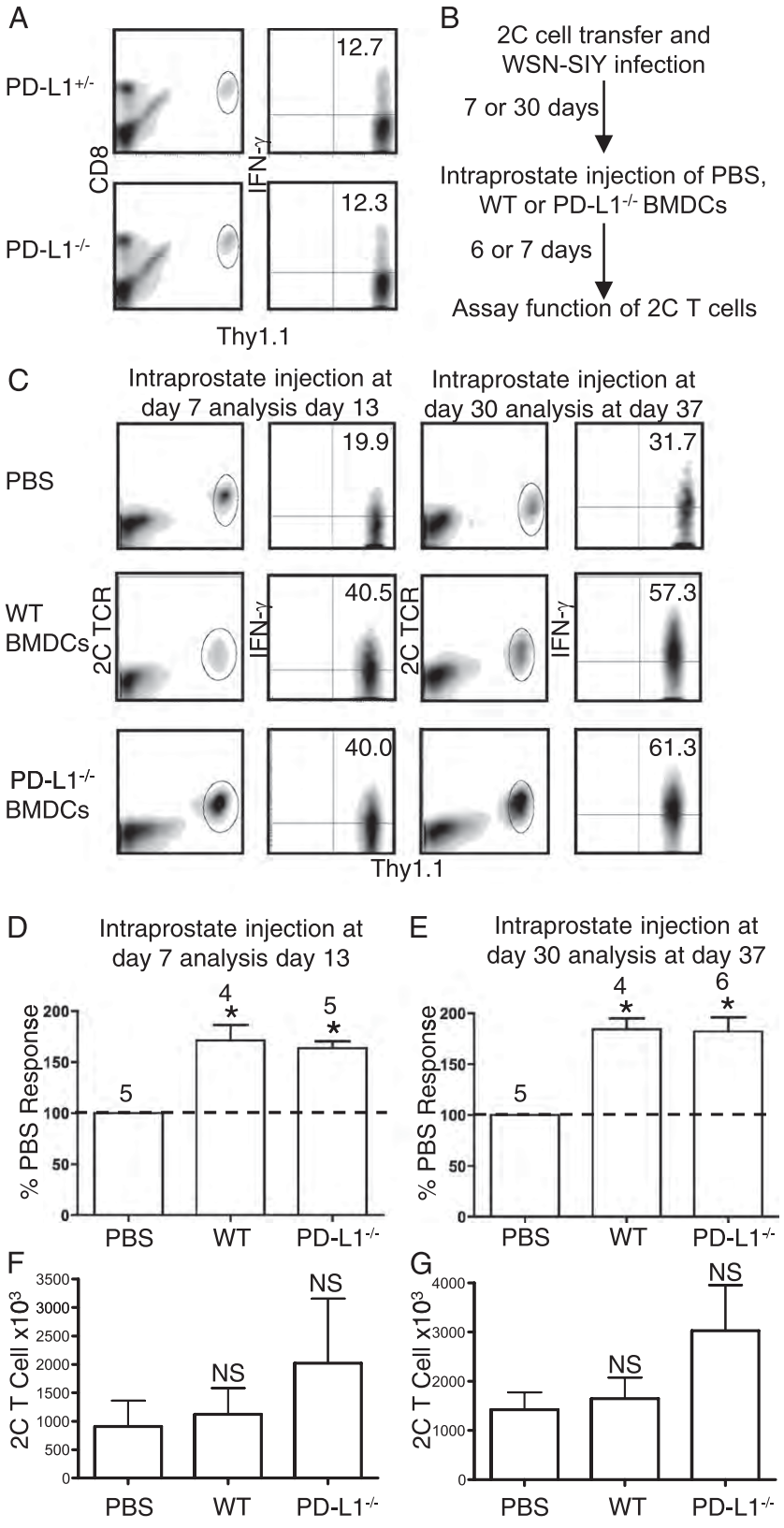

FIGURE 2. Modulation of the PD-1/PD-L1 interaction between 2C T cells and prostate or BMDCs does not affect T cell activity. (**A**) Naive 2C T cells were transferred into PD-L1$^{+/-}$ or PD-L1$^{-/-}$ TRP-SIY mice, along with intranasal infection with WSN-SIY virus. On day 14, 2C T cells were harvested from prostate tissue, stimulated with SIY peptide, and analyzed for IFN-γ expression. CD8 versus Thy1.1 plots were gated on all live cells from prostate. IFN-γ versus Thy1.1 plots were gated on CD8$^+$ Thy1.1$^+$ cells. Representative FACS plots from three experiments are shown. (**B**) Experimental scheme for analyzing BMDC-mediated delay of tolerance induction and refunctionalization of tolerized 2C cells in the prostate of TRP-SIY mice. On day 0, naive 2C T cells were adoptively transferred into TRP-SIY mice and given intranasal infection with WSN-SIY virus. On day 7 or 30, mice were injected intraprostatically with PBS or 1×10^6 ex vivo matured SIY-loaded wild-type (WT) or PD-L1$^{-/-}$ BMDCs. At 6–7 d later, 2C T cells were harvested from prostate tissue, stimulated with SIY peptide and analyzed for IFN-γ expression. (**C**) Representative plots of flow cytometry analyses of cells from prostate tissues of mice that were injected with PBS, wild type (WT), or PD-L1$^{-/-}$ BMDCs on either day 7 or day 30 after initial 2C cell transfer. 2C TCR versus Thy1.1 plots were gated on all live cells from prostate. IFN-γ versus Thy1.1 staining was gated on 2C TCR$^+$ Thy1.1$^+$ cells. The numbers indicate percentage of IFNγ$^+$ cells. (**D** and **E**) Percentages (mean ± SD) of IFN-γ$^+$ 2C cells from three independent experiments normalized to PBS control. Number of mice for each treatment are indicated. *$p < 0.05$ comparing DC versus PBS injection. (**F** and **G**) Number of 2C TCR$^+$Thy1.1$^+$ cells from prostates injected with PBS, WT, or PD-L1$^{-/-}$ BMDCs either 7 d (F) or 30 d (G) after T cell transfer and analyzed after 6 d (F) or 7 d (G) later. Graphs are from three independent experiments, with at least four mice per group. NS, Compared with PBS control.

expression of CD80 and CD86 before intraprostate injection (Fig. 4A). Therefore, we compared the effect of intraprostatic injection of SIY-loaded wild-type DCs and DCs deficient in CD80, CD86, or both in TRP-SIY mice. Experiments were carried out as in Fig. 2B, except SIY-loaded BMDCs from CD80$^{-/-}$, CD86$^{-/-}$, or CD80$^{-/-}$CD86$^{-/-}$ mice were injected 7 d after initial T cell transfer and WSN-SIY infection. Injection of SIY-loaded wild-type BMDCs, compared with PBS injection, stimulated 2C T cells to express IFN-γ (Fig. 4B). Surprisingly, intraprostatic injection of BMDCs from CD80$^{-/-}$, CD86$^{-/-}$, or CD80$^{-/-}$ CD86$^{-/-}$ mice prolonged IFN-γ expression of infiltrating 2C T cells to a comparable extent, suggesting that neither CD80 nor

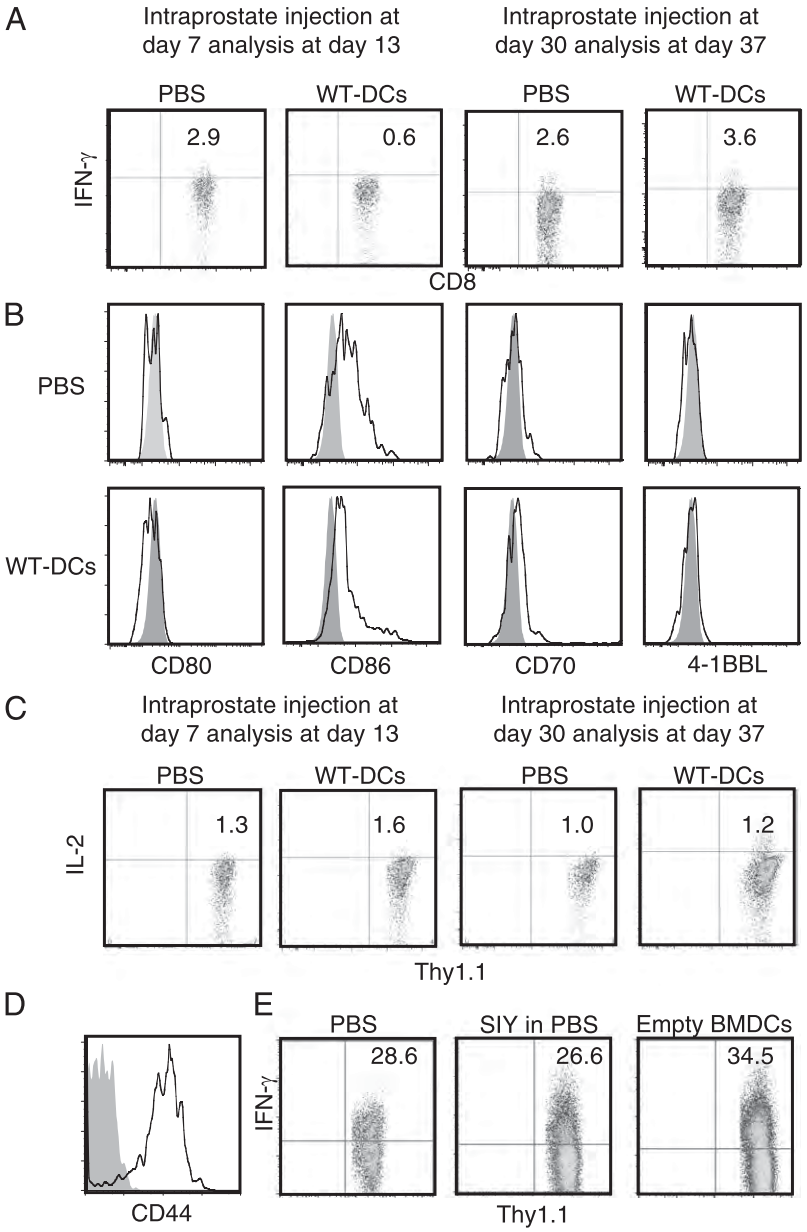

FIGURE 3. BMDCs act directly on 2C T cells in the prostate tissue. (**A**) TRP-SIY mice were injected intraprostatically with PBS- or SIY-loaded wild-type (WT) BMDCs on either day 7 or day 30 after initial 2C cell transfer and infection. At 6–7 d later, Thy1.1$^-$ CD8$^+$ T cells were harvested from prostate tissue and analyzed for IFN-γ expression. IFN-γ versus CD8 plots were gated on live CD8$^+$ Thy1.1$^-$ cells. The numbers indicate percentage of IFN-γ$^+$ cells. (**B**) TRP-SIY mice were injected with PBS or WT-DCs in the prostate. At 6 d later, prostate tissues were dissociated, and single-cell suspensions were stained with CD11c and CD80, CD86, CD70, 4-1BBL (black line), or isotype control (filled gray line). Histograms are gated on live CD11c$^+$ cells. (**C**) TRP-SIY mice were injected with PBS- or SIY-loaded WT BMDCs on either day 7 or day 30 after initial 2C cell transfer and infection. At 6–7 d later, Thy1.1$^+$ 2C T cells were harvested from prostate tissue, stimulated with SIY peptide, and analyzed for IL-2 expression. IFN-γ versus Thy1.1 flow cytometry plots were gated on live 2C TCR$^+$ Thy1.1$^+$ cells. The numbers indicate percentage of IL-2$^+$ cells. (**D**) 2C T cells recovered from the prostates of TRP-SIY were assayed for CD44 expression 13 d post transfer and infection with WSN-SIY virus. Histograms are gated on Thy1.1$^+$2C TCR$^+$ T cells with either CD44 (black line) or isotype (filled gray line) and representative of three independent experiments. (**E**) TRP-SIY mice were injected with PBS, SIY peptide, or LPS-activated wild type (WT) BMDCs not pulsed with SIY peptide 7 d after initial 2C cell transfer and infection. At 6 d later, Thy1.1$^+$ 2C T cells were harvested from prostate tissue, stimulated with SIY peptide, and analyzed for IFN-γ expression. IFN-γ versus Thy1.1 flow cytometry plots were gated on live 2C TCR$^+$ Thy1.1$^+$ cells. The numbers indicate percentage of IFNγ$^+$ cells.

CD86 is required for DC-mediated delay of tolerance induction in prostate tumor tissue.

In addition to their importance in T cell primary responses, CD80 and CD86 are vital for simulating productive secondary responses (18, 19). To determine the requirement for CD80 and/or CD86 in DC-mediated refunctionalization of persisting tolerized T cells in the prostate tumor tissue, we injected SIY-loaded DCs from wild-type, CD80$^{-/-}$, CD86$^{-/-}$, or CD80$^{-/-}$CD86$^{-/-}$ mice 30 d after initial 2C cell transfer and WSN-SIY infection. Compared with PBS control, intraprostatic injection of SIY-loaded wild-type BMDCs reactivated tolerized T cells to express IFN-γ (Fig. 4C). Although injection of SIY-loaded CD86$^{-/-}$ BMDCs stimulated a similar percentage of 2C cells to express IFN-γ in the prostate tumor tissue, the percentage of 2C cells induced to express IFN-γ was significantly reduced following injection of SIY-loaded CD80$^{-/-}$ BMDCs. Most dramatically, the ability of SIY-loaded BMDCs to induce 2C cell expression of IFN-γ was completely abrogated by deficiency of CD80 and CD86. These results suggest that although deficiency of CD86 can be compensated by the presence of CD80, CD80 deficiency cannot be completely compensated by the presence of CD86. Thus, CD80 is critical for DC-mediated refunctionalization of tolerized T cells in the prostate tumor tissue.

The requirement of CD80 and CD86 in reactivating tolerized T cells in tumor tissue was further supported by an in vivo cytotoxicity assay. At 30 d after initial 2C T cell transfer into, and infection of, TRP-SIY mice and 6 d after injection of PBS or BMDCs, CFSE^{Hi} SIY pulsed target cells and CFSE^{Lo} control target cells, at a 1:1 ratio, were transferred into the mice. Approximately 24 h later, the ratio of CFSE^{Hi} to CFSE^{Lo} cells in the prostate was determined by flow cytometry to assess the level of Ag-specific target cell lysis. When wild-type BMDCs were injected, only 8% of CFSE^{Hi} target cells remained compared with 30% in PBS-injected prostates (Fig. 4D). When CD80$^{-/-}$ or CD80$^{-/-}$CD86$^{-/-}$ BMDCs were injected, 21% and 30% of CFSE^{Hi} target cells remained, respectively. These results suggest that deficiency of CD80 and CD86 impairs the ability of Ag-loaded DCs to reactivate tolerized 2C cells in prostate tumor tissue.

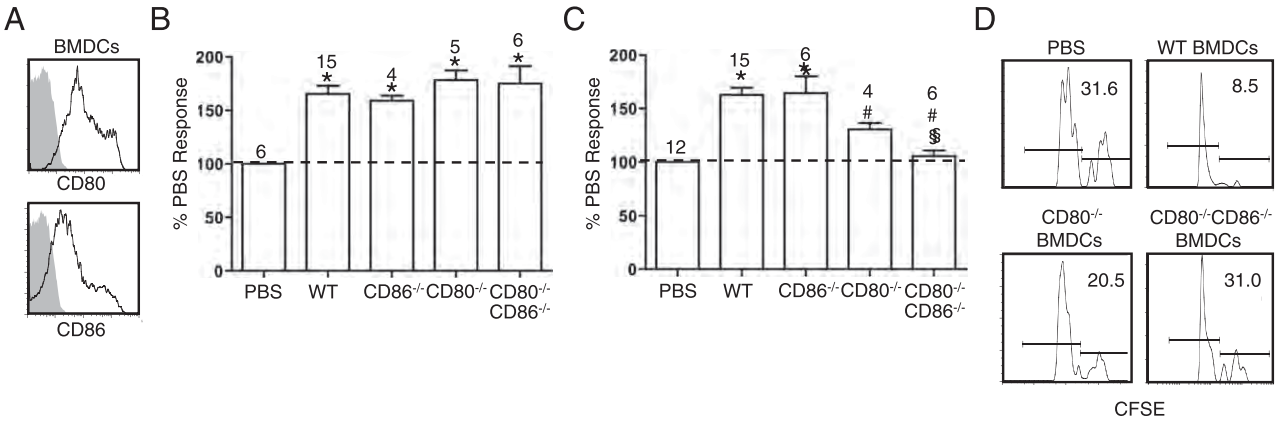

FIGURE 4. CD80 and CD86 expression on BMDCs is necessary for 2C T cell reactivation, but not the delay of 2C T cell tolerance. (**A**) Day 7 LPS-activated BMDCs were stained with anti-CD11c, -CD80, or -CD86 Abs (black line) or isotype control (filled gray line). CD80 and CD86 expression histograms are gated on $CD11c^+$ cells. (**B** and **C**) Mice were treated and cells analyzed as in Fig. 2B, with prostate tissues injected with PBS, wild-type (WT), $CD80^{-/-}$, $CD86^{-/-}$, or $CD80^{-/-}CD86^{-/-}$ BMDCs on either (B) day 7 or (C) day 30 after initial 2C cell transfer and infection. Percentages (mean ± SD) of IFN-γ^+ 2C cells from at least three independent experiments are normalized to PBS control. Number of mice for each treatment is indicated. $^*p < 0.05$, comparing DC with PBS injection, $^{\#}p < 0.05$ comparing WT with knockout DCs, $^{\S}p < 0.05$ comparing $CD80^{-/-}CD86^{-/-}$ DCs with $CD80^{-/-}$ DCs. (**D**) At 30 d post 2C cell transfer and infection, TRP-SIY mice were injected intraprostatically with PBS, or SIY-loaded WT, $CD80^{-/-}$, $CD80^{-/-}/CD86^{-/-}$ BMDCs. On day 36, mice were injected retro-orbitally with a 1:1 mixture of SIY-pulsed ($CFSE^{Hi}$) and unpulsed ($CFSE^{Lo}$) activated T cells ($Thy1.1^+$). The following day, the proportions of $CFSE^{Hi}$ versus $CFSE^{Lo}$ target cells were determined by flow cytometry. CFSE histograms are shown for live $Thy1.1^+$ cells. Numbers indicate percentage of $CFSE^+$ cells. Representative data from one of the two experiments are shown.

CD70, but not 4-1BBL, is required for BMDC-mediated delay in T cell tolerance

CD86 and CD80 do not affect the ability of BMDCs to delay 2C T cell tolerance, indicating other costimulatory molecules may potentiate these effects. TNF costimulatory molecules, such as 4-1BBL and CD70, promote T cell activation during initial priming and may be important for 2C T cell function during initial infiltration within the prostate tissue (8). For example, engagement of 4-1BB on $CD8^+$ T cells by 4-1BBL enhances T cell cytotoxic function (20, 21). Similarly, CD70 functions to maintain T cell survival and proliferation in the periphery (22, 23). Activated BMDCs express higher levels of CD70 and 4-1BBL relative to the expression on endogenous prostate DCs (Fig. 5A, compared with Fig. 3B). We used anti-CD70 and anti–4-1BBL Abs previously shown to block CD70/CD27 and 4-1BBL/4-1BB interactions in vivo, to define the contribution of CD70 and 4-1BB in DC-mediated delay of tolerance induction (14, 24). To exclude possible FcR-mediated effect on the DCs, we generated an $F(ab')_2$ fragment of each Ab lacking the Fc portion of the molecule but still retaining binding activity, as assessed by the ability to compete with fluorescently labeled full-length Ab for cell surface binding (Fig. 5B). As a control, we used $F(ab')_2$ of the Ab mixture against FcRs CD16 and CD32 (25). SIY-loaded BMDCs were incubated with each Ab fragment and then injected into prostate tumor tissue of TRP-SIY mice 7 d after 2C T cell transfer and WSN-SIY infection. FcR-blocking Abs did not diminish the ability of BMDCs to stimulate prolonged IFN-γ expression by infiltrating 2C T cells (Fig. 5C). Blocking the interaction between 4-1BB on 2C T cells and 4-1BBL on BMDCs did not impair the ability of DCs to extend IFN-γ expression by infiltrating 2C T cells. However, blockade of CD70 on BMDCs significantly reduced their ability to stimulate prolonged IFN-γ expression by infiltrating 2C T cells in the prostate (Fig. 5C). The observed difference was not due to differential retention of anti-CD70–treated BMDCs within prostate tissue, compared with control-treated BMDCs (Fig. 5E), consistent with previous experiments with untreated BMDCs (13). These results show that CD70/CD27 interaction is required for DC-mediated delay of 2C T cell tolerance induction in prostate tumor tissue.

As 4-1BBL and CD70 have been shown to enhance recall responses and reactivate previously tolerized T cells (26, 27), we examined the effect of 4-1BBL and CD70 on reactivation of already tolerized 2C T cells. We injected Ab-treated, SIY-loaded BMDCs into the prostate of TRP-SIY mice 30 d after 2C T cell transfer and WSN-SIY infection. Blockade of either CD70 or 4-1BBL did not significantly reduce the fractions of persisting 2C T cells that were induced to express IFN-γ (Fig. 5D), indicating that CD70 and 4-1BBL are not required for reactivation of tolerized 2C T cells in prostate tumor tissue.

CD27 is downregulated on prostate resident T cells

The costimulatory molecules necessary to delay tolerance induction and reactivate already tolerized 2C T cells are distinct. BMDCs expressed similar levels of costimulatory molecules, whether they were used to delay tolerance induction or reactivate already tolerized T cells. The functional differences between these two time points may be a result of phenotypic changes on prostate resident 2C T cells. Thus, we assessed 2C T cell expression of CD28, CD27, and 4-1BB before transfer and 13, 23, and 36 d following transfer and infection in TRP-SIY mice. CD28 expression on 2C T cells from prostate remained similar at the three different time points and was similar to that of naive 2C T cells (Fig. 6A–C). The expression of 4-1BB was low on 2C T cells recovered from TRP-SIY prostate throughout the 36 d following transfer (Fig. 6B, 6C). CD27 was highly expressed on naive 2C T cells (Fig. 6A). In contrast to CD28 and 4-1BB, expression of CD27 was progressively lost from 2C T cells following infiltration into TRP-SIY prostate tissue (Fig. 6B, 6C). To determine if CD27 downregulation is specific to the TRP-SIY prostate, we transferred 2C T cells into TRAMP and C57BL/6 mice. As shown in Fig. 6D, CD27 expression on 2C T cells was also downregulated on the prostate of TRAMP and C57BL/6 mice. The observed downregulation is specific to the prostate, as the level of CD27 on 2C T cells from spleen of the same mice remained stable (Fig. 6E). These results show that the lack of effect of anti-CD70 treatment during reactivation is correlated with the downregulation of CD27 on persisting tolerized 2C T cells in the prostate.

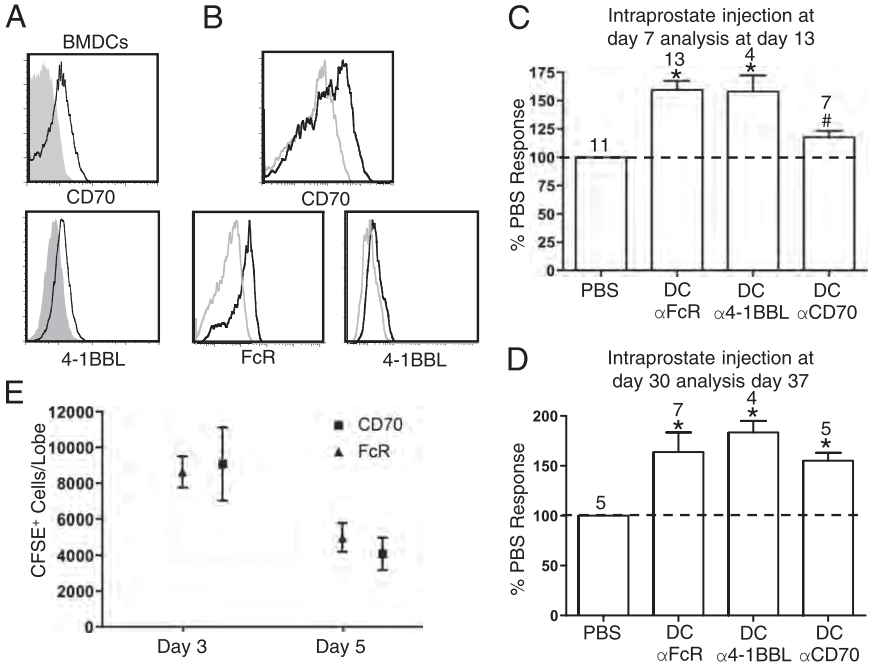

FIGURE 5. CD70 is required for DC-mediated delay in 2C T cell tolerance. (**A**) Day 7 LPS-activated BMDCs were stained for CD11c plus CD70, 4-1BBL (black line), or isotype control (filled gray line). Histograms are gated on $CD11c^+$ cells. (**B**) $F(ab')_2$ fragments are confirmed to maintain their Ag-binding capacity using a competition assay. BMDCs were incubated with 10 μg/ml of fluorescently labeled full-length Ab in the presence of the same amount of either $F(ab')_2$ of interest or control anti-FcR $F(ab')_2$ fragment. The cells were then stained with anti-CD11c and analyzed by flow cytometry. Center histogram shows binding of fluorescently labeled anti-CD70 to BMDCs in the presence of either anti-CD70 $F(ab')_2$ (gray) or control anti-FcR $F(ab')_2$ (black). *Left* histogram shows binding of fluorescently labeled anti-CD16/CD32 to BMDCs in the presence of either anti-FcR $F(ab')_2$ (gray) or control anti-CD70 $F(ab')_2$ (black). *Right* histogram shows binding of fluorescently labeled anti–4-1BBL to BMDCs in the presence of either anti–4-1BBL $F(ab')_2$ (gray) or control anti-FcR $F(ab')_2$ (black). Histograms are gated on $CD11c^+$cells. (**C**) Experiments were conducted as in Fig. 2B with SIY-pulsed BMDCs incubated with anti-FcR, CD70, or 4-1BBL $F(ab')_2$ fragments. Shown are percentages (mean ± SD) of IFN-γ^+ 2C cells from three independent experiments normalized to PBS control. Number of mice for each treatment is indicated. (**D**) As in (C), except BMDCs were injected on day 30 post T cell transfer, and analysis was carried out on day 37. Shown are percentages (mean ± SD) of IFN-γ^+ 2C cells from three independent experiments normalized to PBS control. Number of mice for each treatment is indicated. $^*p < 0.05$ comparing DC with PBS injection, $^{\#}p < 0.05$ comparing BMDCs treated with anti-CD70 $F(ab')_2$ and those treated with anti-FcR $F(ab')_2$. (**E**) Day 7 LPS-matured BMDCs were labeled with CFSE and incubated with $F(ab')_2$ fragments specific for FcR or CD70. DCs (10×10^3 per mouse) were surgically injected into one of the dorsal prostate lobes. At 3 and 5 d later, mice were sacrificed, and $CSFE^+$ DCs in each of the prostate tissues were assessed by flow cytometry. Shown are the average numbers of DCs (±SD) from three prostates per group, per time point.

Discussion

Molecular interactions that underlie the ability of DCs to overcome tumor-induced T cell tolerance are largely unknown. In an autochthonous model of prostate cancer, we have previously defined two stages at which activated DCs can overcome tumor microenvironment: delaying tolerance induction of tumor-infiltrating T cells and reactivating already tolerized T cells in the tumor tissue. In this study, we have now identified molecules necessary for the effects of DCs. Our data show that CD70/CD27 interaction between T cells and BMDCs is required for DC-mediated delay in 2C T cell tolerance. Our study further refines the role of CD70 by demonstrating that CD70/CD27 interaction can sustain intratumoral T cell activity in an otherwise tolerizing environment. Previous reports of CD70 function in tumor models have been restricted to transplantable cell lines. Overexpression of CD70 by endogenous APCs enhances priming of T cells against the EL4-NP and B6F10 tumor cell lines (9, 28). Furthermore, activation of clonotypic T cells with an anti-CD27 Ab enhances the rejection of another transplantable melanoma cell line (29). These studies focus on priming of anti-tumor T cells in transplantable tumor models. In contrast, we analyze the requirement of costimulatory molecules to overcome tolerization in an autochthonous prostate model. Studies have shown that provision of Ag-specific CD4 T cells to TRAMP mice sustains SV40-specific CD8 T cell function through CD40L activation of endogenous DCs (30). As CD40L stimulation promotes CD70 expression on DCs (31), CD70-dependent signals from DCs may be a common pathway to activate prostate tumor-reactive T cells. Notably, CD80, CD86, and 4-1BBL do not play a direct role in delaying prostate tumor-induced T cell tolerance, perhaps because they do not influence CD70 expression.

The CD80 and CD86 costimulatory molecules are best known for their role in naive T cell activation. Our results presented in this study demonstrate that CD80 is also required to reactivate tolerized T cells in prostate tumor tissue. It is notable that $CD86^{-/-}$ DCs are as potent as wild-type DCs in reactivating tolerized T cells. $CD80^{-/-}$ DCs exhibit a significantly reduced ability to reactivate tolerized T cells, and this function is completely abolished when combined with CD86 deficiency. These results reveal distinct functions for CD80 and CD86 in DC-mediated reactivation of tolerized T cells. In contrast, blocking CD70 or 4-1BBL does not affect the ability of DCs to reactivate tolerized 2C T cells. This finding is perhaps explained by the lack of CD27 and low 4-1BB expression on persisting T cells in the TRP-SIY prostate. These findings highlight the spatiotemporal specificity of costimulatory molecules in augmenting tumor-specific T cell responses.

Our studies demonstrate that the ability of BMDCs to overcome T cell tolerance is based on a combination of Ag specificity and costimulation. Despite Ag expression within the TRP-SIY prostate (11), and a population of tissue resident DCs (13), 2C T cells are

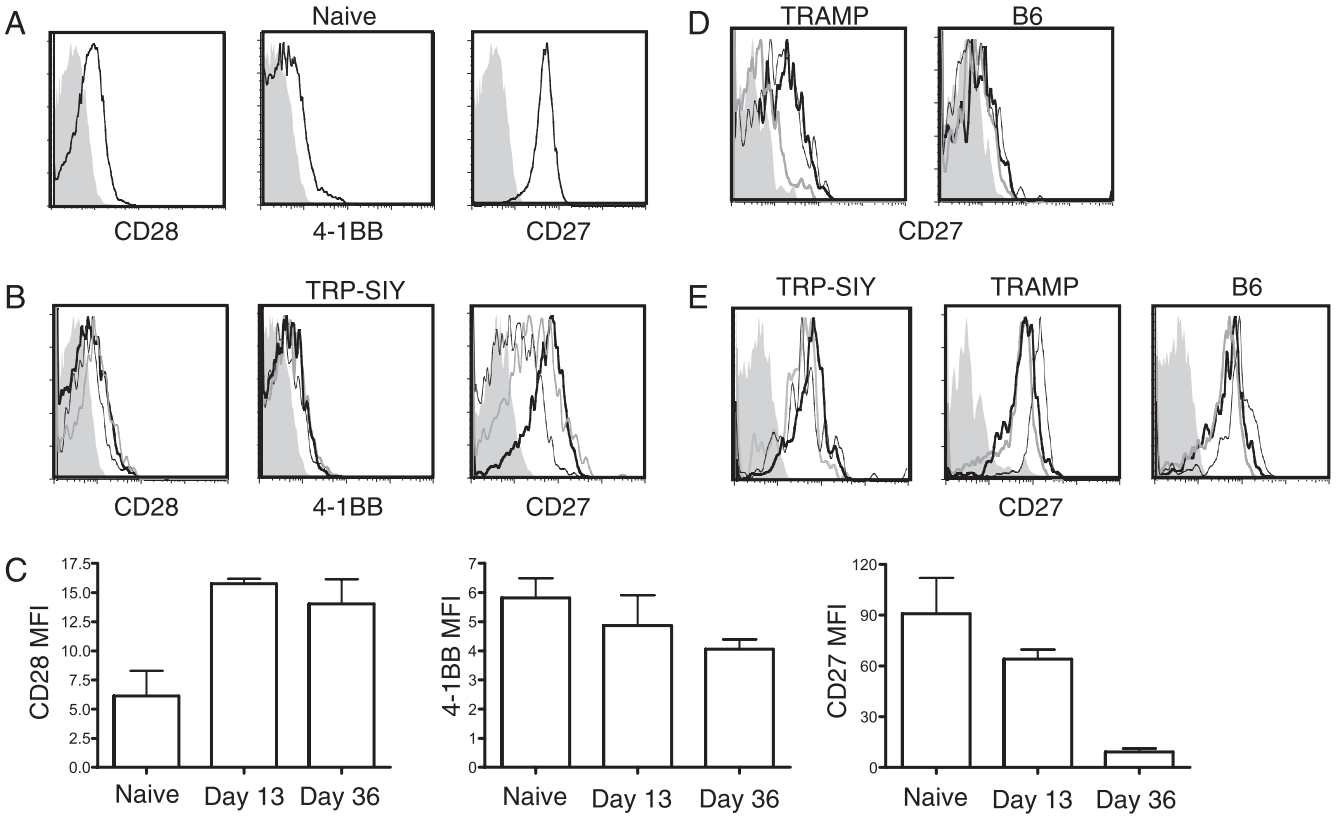

FIGURE 6. CD27 expression is progressively lost on TRP-SY prostate resident 2C T cells. (**A**) Naive 2C T cells pooled from spleens and lymph nodes were assayed for expression of CD28, 4-1BB, and CD27. Histograms are gated on Thy1.1$^+$ 2C TCR$^+$ cells stained with isotype Ab (shaded gray) or specific Ab (black line). (**B**) Naive Thy1.1$^+$ 2C T cells were retro-orbitally injected into TRP-SIY mice, along with intranasal infection with WSN-SIY virus. Mice were sacrificed 13 (bold black line), 23 (gray line), and 36 (thin black line) d post transfer, and CD28, 4-1BB, and CD27 expression on prostate resident 2C T cells was assayed by flow cytometry. Histograms are gated on live 2C TCR$^+$ Thy1.1$^+$ cells with isotype Ab (shaded gray) or specific Ab (black line). (**C**) Mean fluorescence intensity of CD28, CD27, or 4-1BB staining from Thy1.1$^+$2C TCR$^+$ T cells from naive mice or recovered from prostates at indicated times post transfer and WSN-SIY infection. Data shown are from at least two independent experiments (mean ± SD). (**D**) Time course of CD27 expression on 2C T cells recovered from TRAMP and C57BL/6 (B6) prostates 13 (bold black line), 23 (gray line), and 36 (thin black line) d post transfer. (**E**) As above, with 2C transfer/WSN-SIY infection and analysis of CD27 on 2C TCR$^+$Thy1.1$^+$ 2C T cells 13 (bold black line), 23 (gray line), and 36 (thin black line) d post transfer in spleens from TRP-SIY, TRAMP, and B6 mice.

tolerized within the prostate. Indeed, we show that endogenous DCs within the prostate express levels of costimulatory molecules barely above background (Fig. 3B). Previous work has shown that depletion of prostate DCs reverses 2C T cell tolerance (13). Considering that tolerance can result from pMHC presentation by DCs lacking costimulatory signals (32), these data suggest that steady-state prostate resident DCs promote T cell tolerance, perhaps through pMHC/TCR engagement without costimulation. However, when peptide-pulsed, LPS-activated, BMDCs are injected into the prostate, 2C T cells are reactivated in a CD70 or CD80/CD86-dependent manner. The injection of activated BMDCs may provide a costimulatory signal that is normally lacking in the TRP-SIY prostate. This notion is supported by three lines of evidence. First, we have demonstrated that 2C T cell reactivation is dependent on the interaction between costimulatory receptors and ligands (Figs. 4, 5). Second, LPS-activated BMDCs without SIY peptide activate a greater percentage of 2C T cells, compared with PBS injection, but less than SIY pulsed LPS activated DCs. This observation suggests that enough residual SIY peptide is present in the prostate to be acquired and presented by activated BMDCs, and further highlights the importance of the pMHC/TCR interaction. Third, the window in which 2C T cells remain activated in this model directly depends on the presence of BMDCs within the prostate (13), reinforcing the importance of the presence of costimulatory molecules.

In addition to stimulatory molecules, 2C T cells within the prostate express high levels of the inhibitory receptor PD-1. In human patients and mouse models of cancer, T cells express PD-1, Tim3, and LAG3 individually or in combination, depending on tumor type (16, 33, 34). We find tumor-infiltrating 2C T cells express, and maintain, uniformly high levels of PD-1 but do not express Tim3 or LAG3. Despite the expression of PD-L1 within the tumor islets of the TRP-SIY prostate, genetic deletion of PD-L1 on the TRP-SIY background did not inhibit the induction of T cell tolerance in prostate tumor tissue. This finding indicates that PD-1 is not critical for tolerance induction, but is perhaps a marker of exhausted T cells, similar to dysfunctional T cells in chronic viral infections (35). Furthermore, PD-L1$^{-/-}$ BMDCs were as active as wild-type DCs in reactivating tolerized 2C T cells in prostate tumor tissue. This unexpected finding is seemingly at odds with the literature outlining the increase in tumor-associated T cell function after blockade of PD-1 (5, 36). The specifics of our model system likely account for these differences. We note that in many systems restoration of tumor tolerized T cell function requires blockade of multiple inhibitory pathways to regain full function (16, 33, 37). As we found that 2C T cells upregulate PD-1 and not LAG-3 or Tim3, there may be additional, unidentified coinhibitory receptors functioning in this system. Further, inefficacy of PD-L1 blockade in the context of BMDC injection may be a consequence of the powerful stimulatory capacity of DCs. BMDCs may provide

the maximal stimulation of tolerized T cells regardless of PD-1/PD-L1 engagement. This highlights the tissue (TRP-SIY prostates) and context (DC-mediated reactivation) specificity in the utility of checkpoint blockades in tumor resident T cell activity.

In summary, the differential requirement for CD70 and CD80/CD86 in T cell function within the tumor environment suggests approaches to enhance ACT- and DC-based vaccines for cancer immunotherapy. For example, enhancing the CD27/CD70 interaction may delay tolerization of adoptively transferred T cells in the tumor microenvironment, and enhancing CD80 expression by DCs could stimulate anti-tumor response by endogenous tolerized $CD8^+$ T cells. Defining the molecular interactions necessary to overcome tumor-induced tolerance is critical, as provision of costimulatory Fc fusion proteins, transduction of whole-cell tumor vaccines with costimulatory molecules, and viral vectors expressing costimulatory molecules are under development for the treatment of tumors (2). Our findings provide a basis for the rational design of ACT and DC vaccines targeting tumor-specific immune responses.

Acknowledgments

We thank Camille Jusino, Carol McKinley, Marisha Mikell, and the Swanson Biotechnology Core Facility at the Koch Institute for technical support; members of the Chen Lab for helpful discussions; and Dr. Arlene Sharpe (Harvard Medical School, Boston, MA) and Dr. Leiping Chen (Yale University, New Haven, CT) for CD80 and PD-L1 knockouts, respectively.

Disclosures

The authors have no financial conflicts of interest.

References

1. Rosenberg, S. A., N. P. Restifo, J. C. Yang, R. A. Morgan, and M. E. Dudley. 2008. Adoptive cell transfer: a clinical path to effective cancer immunotherapy. *Nat. Rev. Cancer* 8: 299–308.
2. Gulley, J. L., and C. G. Drake. 2011. Immunotherapy for prostate cancer: recent advances, lessons learned, and areas for further research. *Clin. Cancer Res.* 17: 3884–3891.
3. Sharpe, A. H. 2009. Mechanisms of costimulation. *Immunol. Rev.* 229: 5–11.
4. Fife, B. T., and J. A. Bluestone. 2008. Control of peripheral T-cell tolerance and autoimmunity via the CTLA-4 and PD-1 pathways. *Immunol. Rev.* 224: 166–182.
5. Pilon-Thomas, S., A. Mackay, N. Vohra, and J. J. Mulé. 2010. Blockade of programmed death ligand 1 enhances the therapeutic efficacy of combination immunotherapy against melanoma. *J. Immunol.* 184: 3442–3449.
6. Chen, L., P. McGowan, S. Ashe, J. V. Johnston, I. Hellström, and K. E. Hellström. 1994. B7-1/CD80-transduced tumor cells elicit better systemic immunity than wild-type tumor cells admixed with *Corynebacterium parvum*. *Cancer Res.* 54: 5420–5423.
7. Antonia, S. J., J. Seigne, J. Diaz, C. Muro-Cacho, M. Extermann, M. J. Farmelo, M. Friberg, M. Alsarraj, J. J. Mahany, J. Pow-Sang, et al. 2002. Phase I trial of a B7-1 (CD80) gene modified autologous tumor cell vaccine in combination with systemic interleukin-2 in patients with metastatic renal cell carcinoma. *J. Urol.* 167: 1995–2000.
8. Watts, T. H. 2005. TNF/TNFR family members in costimulation of T cell responses. *Annu. Rev. Immunol.* 23: 23–68.
9. Arens, R., K. Schepers, M. A. Nolte, M. F. van Oosterwijk, R. A. van Lier, T. N. Schumacher, and M. H. van Oers. 2004. Tumor rejection induced by CD70-mediated quantitative and qualitative effects on effector CD8+ T cell formation. *J. Exp. Med.* 199: 1595–1605.
10. May, K. F., Jr., L. Chen, P. Zheng, and Y. Liu. 2002. Anti-4-1BB monoclonal antibody enhances rejection of large tumor burden by promoting survival but not clonal expansion of tumor-specific CD8+ T cells. *Cancer Res.* 62: 3459–3465.
11. Bai, A., E. Higham, H. N. Eisen, K. D. Wittrup, and J. Chen. 2008. Rapid tolerization of virus-activated tumor-specific CD8+ T cells in prostate tumors of TRAMP mice. *Proc. Natl. Acad. Sci. USA* 105: 13003–13008.
12. Olurinde, M. O., C. H. Shen, A. Drake, A. Bai, and J. Chen. 2011. Persistence of tumor-infiltrating CD8 T cells is tumor-dependent but antigen-independent. *Cell Mol. Immunol.* 8: 415–423.
13. Higham, E. M., C. H. Shen, K. D. Wittrup, and J. Chen. 2010. Cutting edge: delay and reversal of T cell tolerance by intratumoral injection of antigen-loaded dendritic cells in an autochthonous tumor model. *J. Immunol.* 184: 5954–5958.
14. Van Deusen, K. E., R. Rajapakse, and T. N. Bullock. 2010. CD70 expression by dendritic cells plays a critical role in the immunogenicity of CD40-independent, CD4+ T cell-dependent, licensed CD8+ T cell responses. *J. Leukoc. Biol.* 87: 477–485.
15. Sakuishi, K., P. Jayaraman, S. M. Behar, A. C. Anderson, and V. K. Kuchroo. 2011. Emerging Tim-3 functions in antimicrobial and tumor immunity. *Trends Immunol.* 32: 345–349.
16. Woo, S. R., M. E. Turnis, M. V. Goldberg, J. Bankoti, M. Selby, C. J. Nirschl, M. L. Bettini, D. M. Gravano, P. Vogel, C. L. Liu, et al. 2012. Immune inhibitory molecules LAG-3 and PD-1 synergistically regulate T-cell function to promote tumoral immune escape. *Cancer Res.* 72: 917–927.
17. Zhou, P., X. Zheng, H. Zhang, Y. Liu, and P. Zheng. 2009. B7 blockade alters the balance between regulatory T cells and tumor-reactive T cells for immunotherapy of cancer. *Clin. Cancer Res.* 15: 960–970.
18. Fuse, S., W. Zhang, and E. J. Usherwood. 2008. Control of memory CD8+ T cell differentiation by CD80/CD86-CD28 costimulation and restoration by IL-2 during the recall response. *J. Immunol.* 180: 1148–1157.
19. Habib-Agahi, M., T. T. Phan, and P. F. Searle. 2007. Co-stimulation with 4-1BB ligand allows extended T-cell proliferation, synergizes with CD80/CD86 and can reactivate anergic T cells. *Int. Immunol.* 19: 1383–1394.
20. Shuford, W. W., K. Klussman, D. D. Tritchler, D. T. Loo, J. Chalupny, A. W. Siadak, T. J. Brown, J. Emswiler, H. Raecho, C. P. Larsen, et al. 1997. 4-1BB costimulatory signals preferentially induce CD8+ T cell proliferation and lead to the amplification in vivo of cytotoxic T cell responses. *J. Exp. Med.* 186: 47–55.
21. Lee, H. W., S. J. Park, B. K. Choi, H. H. Kim, K. O. Nam, and B. S. Kwon. 2002. 4-1BB promotes the survival of CD8+ T lymphocytes by increasing expression of Bcl-xL and Bfl-1. *J. Immunol.* 169: 4882–4888.
22. Schildknecht, A., I. Miescher, H. Yagita, and M. van den Broek. 2007. Priming of CD8+ T cell responses by pathogens typically depends on CD70-mediated interactions with dendritic cells. *Eur. J. Immunol.* 37: 716–728.
23. Tesselaar, K., Y. Xiao, R. Arens, G. M. van Schijndel, D. H. Schuurhuis, R. E. Mebius, J. Borst, and R. A. van Lier. 2003. Expression of the murine CD27 ligand CD70 in vitro and in vivo. *J. Immunol.* 170: 33–40.
24. Seko, Y., N. Takahashi, H. Oshima, O. Shimozato, H. Akiba, K. Takeda, T. Kobata, H. Yagita, K. Okumura, M. Azuma, and R. Nagai. 2001. Expression of tumour necrosis factor (TNF) ligand superfamily co-stimulatory molecules CD30L, CD27L, OX40L, and 4-1BBL in murine hearts with acute myocarditis caused by Coxsackievirus B3. *J. Pathol.* 195: 593–603.
25. Kurlander, R. J., D. M. Ellison, and J. Hall. 1984. The blockade of Fc receptor-mediated clearance of immune complexes in vivo by a monoclonal antibody (2.4G2) directed against Fc receptors on murine leukocytes. *J. Immunol.* 133: 855–862.
26. Keller, A. M., A. Schildknecht, Y. Xiao, M. van den Broek, and J. Borst. 2008. Expression of costimulatory ligand CD70 on steady-state dendritic cells breaks CD8+ T cell tolerance and permits effective immunity. *Immunity* 29: 934–946.
27. Bertram, E. M., P. Lau, and T. H. Watts. 2002. Temporal segregation of 4-1BB versus CD28-mediated costimulation: 4-1BB ligand influences T cell numbers late in the primary response and regulates the size of the T cell memory response following influenza infection. *J. Immunol.* 168: 3777–3785.
28. Keller, A. M., Y. Xiao, V. Peperzak, S. H. Naik, and J. Borst. 2009. Costimulatory ligand CD70 allows induction of CD8+ T-cell immunity by immature dendritic cells in a vaccination setting. *Blood* 113: 5167–5175.
29. Roberts, D. J., N. A. Franklin, L. M. Kingeter, H. Yagita, A. L. Tutt, M. J. Glennie, and T. N. Bullock. 2010. Control of established melanoma by CD27 stimulation is associated with enhanced effector function and persistence, and reduced PD-1 expression of tumor infiltrating CD8(+) T cells. *J. Immunother.* 33: 769–779.
30. Shafer-Weaver, K. A., S. K. Watkins, M. J. Anderson, L. J. Draper, A. Malyguine, W. G. Alvord, N. M. Greenberg, and A. A. Hurwitz. 2009. Immunity to murine prostatic tumors: continuous provision of T-cell help prevents CD8 T-cell tolerance and activates tumor-infiltrating dendritic cells. *Cancer Res.* 69: 6256–6264.
31. Bullock, T. N., and H. Yagita. 2005. Induction of CD70 on dendritic cells through CD40 or TLR stimulation contributes to the development of CD8+ T cell responses in the absence of CD4+ T cells. *J. Immunol.* 174: 710–717.
32. Hochweller, K., and S. M. Anderton. 2005. Kinetics of costimulatory molecule expression by T cells and dendritic cells during the induction of tolerance versus immunity in vivo. *Eur. J. Immunol.* 35: 1086–1096.
33. Fourcade, J., Z. Sun, M. Benallaoua, P. Guillaume, I. F. Luescher, C. Sander, J. M. Kirkwood, V. Kuchroo, and H. M. Zarour. 2010. Upregulation of Tim-3 and PD-1 expression is associated with tumor antigen-specific CD8+ T cell dysfunction in melanoma patients. *J. Exp. Med.* 207: 2175–2186.
34. Sakuishi, K., L. Apetoh, J. M. Sullivan, B. R. Blazar, V. K. Kuchroo, and A. C. Anderson. 2010. Targeting Tim-3 and PD-1 pathways to reverse T cell exhaustion and restore anti-tumor immunity. *J. Exp. Med.* 207: 2187–2194.
35. Blackburn, S. D., A. Crawford, H. Shin, A. Polley, G. J. Freeman, and E. J. Wherry. 2010. Tissue-specific differences in PD-1 and PD-L1 expression during chronic viral infection: implications for CD8 T-cell exhaustion. *J. Virol.* 84: 2078–2089.
36. Rosenblatt, J., B. Glotzbecker, H. Mills, B. Vasir, D. Tzachanis, J. D. Levine, R. M. Joyce, K. Wellenstein, W. Keefe, M. Schickler, et al. 2011. PD-1 blockade by CT-011, anti-PD-1 antibody, enhances ex vivo T-cell responses to autologous dendritic cell/myeloma fusion vaccine. *J. Immunother.* 34: 409–418.
37. Fourcade, J., Z. Sun, O. Pagliano, P. Guillaume, I. F. Luescher, C. Sander, J. M. Kirkwood, D. Olive, V. Kuchroo, and H. M. Zarour. 2012. CD8(+) T cells specific for tumor antigens can be rendered dysfunctional by the tumor microenvironment through upregulation of the inhibitory receptors BTLA and PD-1. *Cancer Res.* 72: 887–896.

CD8 T Cell Responses Rapidly Select for Antigen-negative Tumor Cells in the Prostate

S. Peter Bak[*1], Mike Stein Barnkob[*1], K. Dane Wittrup[*‡§], Jianzhu Chen[*†]

[*]Koch Institute for Integrative Cancer Research, [†]Department of Biology, [‡]Biological Engineering, and [§]Chemical Engineering, Massachusetts Institute of Technology, Cambridge, MA 02139, USA

[1]Authors contributed equally to this work

Running Title: T Cells Select for Antigen-negative Tumor Cells in the Prostate

Key Words: Prostate Cancer, T cells, Adoptive Cell Therapy, Immunoediting, Tumor Antigens

Grant Support: This work was partly supported in part by a Postdoctoral Fellowship (12109-PF-11-025-01-LIB) from the American Cancer Society (S.P.B.), the Margaret A. Cunningham Immune Mechanisms in Cancer Research Fellowship (S.P.B.) from the John D. Proctor Foundation, a Prostate Cancer Research Program grant from USAMRMC and Ivan R. Cottrell Professorship and Research Fund (to J.C.), and the Koch Institute Support (core) Grant P30-CA14051 from the National Cancer Institute.

Address correspondence and reprint requests to Jianzhu Chen, Koch Institute for Integrative Cancer Research, Massachusetts Institute of Technology, Cambridge, MA 02139. Tel: 617-258-6173, FAX: 617-258-6172, E-mail address: jchen@mit.edu

Conflict of Interest: None

Word Count: 4,484 **Figures:** 4

Abstract

Stimulation of patients' immune systems for the treatment of solid tumors is an emerging therapeutic paradigm. The use of enriched autologous T cells for adoptive cell therapy (ACT) or vaccination with antigen-loaded dendritic cells have shown clinical efficacy in melanoma and prostate cancer, respectively. However, the long-term effects of immune responses on selection and outgrowth of antigen-negative tumor cells must be determined in order to understand and achieve long term therapeutic effects. In this study, we have investigated the expression of a tumor specific antigen *in situ* after treatment with tumor specific $CD8^+$ T cells in an autochthonous mouse model of prostate cancer. After T cell treatment, aggregates of dead antigen-positive tumor cells were concentrated in the lumen of prostate gland and were eventually eliminated from the prostate tissue. Despite the elimination of antigen-positive tumor cells, prostate tumor continues to grow in T cell treated mice. Interestingly, remaining tumor cells were antigen-negative and downregulated MHC class I expression. These results show that CD8 T cells are effective in eliminating antigen-bearing prostate tumor cells but they also can select for the outgrowth of antigen-negative tumor cells. These findings provide insights into the requirements for an effective cancer immunotherapy: not only inducing potent immune responses but also avoiding selection and outgrowth of antigen-negative tumor cells.

Introduction

A promising cancer immunotherapy is induction of tumor antigen specific CD8 T cell responses. An autologous dendritic cell vaccine targeting prostate acid phosphatase has recently been approved for the treatment of metastatic castration resistant prostate cancer (1). Adoptive cell therapy (ACT), which harvests tumor infiltrating T lymphocytes (TILs), expands them *ex vivo*, and introduces the expanded T cells back to the patient (2), is being developed for treatment of melanoma where strong tumor associated antigens have been described (3). Despite the enormous promise, one potential drawback of antigen-specific cancer immunotherapy is the selection and outgrowth of antigen-negative tumor cells, which can render the immunotherapy ineffective.

Most studies that have examined the selection and outgrowth of antigen-negative tumor cells following induction of tumor-specific CD8 T cell responses have been carried out in animal models. For example, the PA14 antigen (PA14) has been introduced into different tumors, including mastocytomas, plasmocytomas, and fibrosarcomas. When these tumors were transplanted into recipient mice followed with ACT with PA14-specific T cells, antigen loss and tumor outgrowth was observed in all tumor types (4). Similarly, when ovalbumin (OVA)-expressing B16 melanoma cells were transplanted into recipient mice followed with treatment with OVA specific OT-1 CD8 T cells, downregulation of OVA expression was also detected (5, 6). The downregulation of target antigen is not limited to model antigens that were overexpressed in tumor cells. Vaccination of mice transplanted with B16 melanomas induced CD8 T cell responses that selected for tumor cells with downregulated expression of tyrosinase and tyrosinase-related protein 2 antigens (7), suggesting that expression of endogenous tumor antigens are also subject to inhibition as a result of anti-tumor immune responses.

The ability of immune responses to sculpt the antigen repertoire of spontaneously arising tumors is less clear. In a genetically engineered model of melanoma, targeting the gp100 protein with tumor specific T cells led to de-differentiation of melanocytes with concurrent loss of the gp100 antigen (8). Another widely studied autochthonous tumor model is the transgenic adenocarcinoma of the mouse prostate (TRAMP) as a result of prostate-specific expression of

the SV40 large T antigen (Tag). Numerous studies have examined the effect of immunotherapies on TRAMP tumor growth because of the potential of immunotherapy in treating human prostate cancer. However, there has been little analysis on the effect of T cells on antigen expression within TRAMP tumors, and the ability of T cells to select antigen loss variants. A recent study examined the ability of anti-HA T cells to control the growth of prostate tumor in TRAMP mice engineered to express the HA antigen (9). While tumor growth was assessed by prostate weight and histology, there was no examination of antigen expression in the prostate. Similarly, a telomerase vaccine was tested in the TRAMP model and shown to exhibit a protective effect, despite eventual tumor outgrowth (10). While T cell responses, prostate tumor histopathology, and total survival were measured, there was no post-vaccination measurement of target antigen expression (10). Additional studies evaluating the effect of anti-Tag T cells on TRAMP tumors have assessed tumor burden, but have not assessed levels of Tag protein *in situ* (11, 12).

In our study of $CD8^+$ T cell-tumor cell interaction, we have introduced a β-gal-SIY transgene encoding a fusion protein of β-galactosidase with a nominal MHC class I epitope (SIYRYYGL or SIY) recognized by the 2C clonotypic TCR onto the TRAMP mice (TRP-SIY) (13). Adoptive transfer of naïve $CD8^+$ 2C T cells into TRP-SIY mice followed by infection with influenza virus expressing the SIY epitope leads to activation and differentiation of transferred T cells into potent effector cells. As in human patients, effector T cells infiltrate into the prostate tumor tissue and are rapidly tolerized. Similar to human TILs, the 2C T cells persist in the prostate tumor tissue (14) and express high levels of PD-1 (15). This system provides a tractable model to study in detail the effects of adoptively transferred T cells on tumor specific antigen expression. Here, we show that infiltration of activated 2C T cells into the prostate leads to elimination of SIY-positive tumor cells. However, tumor in the prostate of 2C T cell-treated TRP-SIY mice continues to progress with similar kinetics as that in untreated mice. A detailed analysis reveals that all tumor cells in the treated mice are negative for SIY antigen and have also downregulated MHC class I expression. These findings show that CD8 T cells are effective in eliminating antigen-bearing prostate tumor cells but they also select for the outgrowth of antigen-negative tumor cells. These findings shed light on effective cancer immunotherapy that requires not only inducing potent immune responses but also avoiding selection and outgrowth of antigen-negative tumor cells.

Materials and Methods

Mice, Adoptive Transfer and Influenza Infection

TRP-SIY mice were generated as previously described (13). 2C and OT-1 TCR transgenic mice were maintained on C57BL/6 and $RAG1^{-/-}$ backgrounds. Where indicated, mice were retroorbitally injected with $1.5x10^6$ naïve 2C or OT-1 cells from 2C/RAG or OT-1/RAG mice and were intranasally infected with 100 pfu WSN-SIY or WSN-SIIN virus, respectively. Experiments with mice were approved by the Committee on Animal Care (CAC) at Massachusetts Institute of Technology.

Immunohistochemistry

At indicated time points after T cell treatment, the genitourinary tract was excised and all four prostate lobes dissected and flash frozen in OCT compound (Tissue-Tek, Sakura). All tissues were sectioned to 10 μM by the Koch Institute Histology core facility along with matched hematoxylin and eosin (H&E) stained slides. For immunohistochemistry, frozen sections were acetone fixed, blocked with 0.3% H_2O_2 in PBS. Staining was conducted with Vectastain Elite ABC kit (Vector Laboratories) according to the manufacturer's instructions. In some instances slides were stained with X-gal solution (5mM potassium ferricyanide, 2mM magnesium chloride, 1mg/mL X-gal stock solution (Promega) in PBS) for three hours before incubation with primary antibody. Biotinylated antibodies against Thy1.1 (clone HIS51, eBioscience), MHC class I (clone 28-8-6 BD Pharmingen), and CD31 (clone MEC13.3, BioLegend) were visualized with DAB peroxidase staining kit (Vector Labs). Anti-SV40 large T antigen (clone Pab 101, BD Bioscience) staining was conducted with Vectastain Mouse on Mouse Peroxidase Kit (Vector Laboratories), according to the manufacturer's instructions. Where indicated slides were counterstained with eosin (Sigma) or hematoxylin (Vector Labs).

Image and Pathological Analysis

For image analysis, 10 random images were acquired for each sample representing all prostate glands on Zeiss Axioplan II with 10X or 40X objective. For whole mount images, a MIRAX Midi (Carl Zeiss) slide scanner with Axiocam MR(m) camera (Carl Zeiss) was used and images captured using the MIRAX Viewer Software (Carl Zeiss). Peroxidase or β-gal staining was

visualized on each image by thresholding and using preset protocols in Volocity 6.01 (PerkinElmer), such that a precise measurement of area could be made. Total area of gland was determined based on eosin or hematoxylin staining. Contact between stains, as well as luminal and glandular measurements were individually outlined in Velocity and then measured using the preset protocols as above. H&E stained prostate lobes were blindly graded by Dr. Roderick Bronson at the Koch Institute for Integral Cancer Research Pathology Core Facility using the following scale: 0, normal tissue; 1, proliferation with no invasion; 2, early invasion; 3, clear-cut invasion; 4, total replacement of organ.

Statistical Analysis

Data was analyzed with Prism 5.0 (GraphPad Software). Student *t* test was used for comparisons. A p value of less than 0.05 was considered statistically significant. In figures * is indicative of $p < 0.05$, ** $p < 0.01$ and *** $p < 0.001$. Bar graphs represent mean ± standard deviation (SD).

Results

Prostate infiltrating T cells gradually lose contact with antigen-expressing tumor cells

To determine the localization of tumor infiltrating T cells relative to antigen expressing cells in the prostate tumor tissue, we developed an immunohistochemistry analysis for 2C T cells by staining for Thy1.1 (brown) and antigen (SIY)-expressing cancer cells by X-gal staining (blue) for β-galacatosidase (β-gal) in the prostate tumor tissue. In agreement with previous flow cytometry analysis (13), Thy1.1$^+$ 2C T cells were found in the prostate gland 11 days post transfer (dpt) (Fig. 1A). To quantify the Thy1.1 signal, we determined the total area stained by Thy1.1 as a function of the total glandular area stained by eosin (Fig. 1B). Thy1.1 staining area (level) covered approximately 10% of the prostate tumor tissue 11 dpt (Fig. 1B). However, by 35 to 50 dpt, the levels of 2C T cell staining decreased by 75%. These results match the kinetics of T cell levels in TRP-SIY prostates as quantified by flow cytometry analysis of dissociated tissues (13).

To determine whether 2C T cells were in contact with antigen-expressing tumor cells in the prostate tumor, Thy1.1$^+$ staining was separated into categories based on relative distance from the antigen (β-gal) staining. Contiguous staining of Thy1.1 and β-gal was considered as

direct contact between 2C T cells and SIY-expressing tumor cells (Fig. 1C, center top). Thy1.1 signal was further categorized into staining within antigen positive glands but not in direct contact with antigen (Fig. 1C, top right), staining within antigen negative glands (Fig. 1C, lower left), staining outside of the glandular area in the interstitial space (Fig. 1C, center bottom), and staining within the luminal space of the prostate gland (Fig. 1C, lower right). We used this analysis to quantify the changes of 2C T cells within the prostate at 11, 35 and 50 dpt and expressed each category as a fraction of total Thy1.1 signal across the three time-points (Fig. 1D). At 11 dpt approximately 15% of 2C T cells were in direct contact with SIY-expressing cells, with the majority of cells residing within antigen positive prostate glands. By 35 dpt only 5% of 2C T cells were in contact with SIY-expressing cells, although the majority still resided in the antigen positive glands. After 50 dpt, however, very few 2C T cells were in contact with SIY-expressing cells or resided in the antigen positive glands. Associated with the gradual loss of T cell/antigen contact, the proportion of Thy1.1$^+$ 2C T cells in the β-gal$^-$ gland increased. These data show that over time tumor-infiltrating (2C) T cells gradually lose contact with antigen (SIY)-expressing tumor cells in the prostate tissue.

T cell treatment leads to loss of antigen-expressing tumor cells in the prostate

To determine whether the decrease in T cell/antigen contact within the prostate tissue was due to loss of antigen expression over time, we harvested prostate tissues from age-matched TRP-SIY mice with (treated) or without (untreated) 2C T cell transfer/infection, stained tissue sections for β-gal and quantified the percentage of β-gal staining as a function of total prostate glandular area. TRP-SIY prostates normally contain large areas of epithelia that stained positive for β-gal (Fig. 2A, left). Eleven days after 2C T cell treatment, the percentage of β-gal positive areas did not change significantly (Fig. 2A and B). However, by 35 and 50 dpt the level of antigen expression was reduced significantly. The loss of SIY-expressing cells was antigen specific as transfer of OT-1 T cells that recognize SIINFEKL (SIIN) epitope and infection with WSN virus that expresses the SIIN epitope (WSN-SIIN) did not induce the loss of β-gal-expressing cells within the prostates of TRP-SIY mice (Fig. 2B).

We noticed the spatial distribution of X-gal staining was markedly different between untreated and 2C T cell-treated mice 11 dpt. In untreated mice, β-gal staining was spread throughout the

prostate tissue (Fig. 2A, top) and over 90% of staining was found in glandular epithelia (Fig. 2C). In contrast, in the treated mice ~80% β-gal staining was found in the lumen of prostate glands. To determine whether the luminal β-gal positive areas contained viable cells, we compared consecutive sections of tissue stained with either hematoxylin and eosin (H&E) or X-gal. Luminal areas that stained positive for β-gal after T cell treatment were composed of hematoxylin (nuclear stain) negative and eosin positive (cytoskeleton) cellular debris (Fig. 2D). Furthermore, β-gal stains were also detected in the urethra of treated mice (data not shown). These data suggests that the loss of β-gal-expressing tumor cells are likely due to elimination by infiltrating antigen-specific 2C T cells and the mass of dead tumor cells are cleared through the luminal space.

The Presence of 2C T cells within the prostate leads to a reduced expression of MHC class I

Immune responses within the tumor environment can affect antigen expression as well as molecules involved in antigen presentation, particularly MHC class I (16, 17). To determine if 2C T cell treatment of TRP-SIY mice reduces the MHC I expression within prostate tissue, we stained prostate sections from treated and untreated TRP-SIY mice for MHC I expression (Fig. 3A), and quantified the expression as a fraction of total prostate tissue area (Fig. 3B). Eleven days after 2C T cell treatment MHC I expression in treated and untreated mice was similar (Fig. 3B). By 35 dpt two of the four treated mice contained a similar percentage of MHC I^+ tissue area as untreated mice while the other two mice had much reduced percentage. By 50 dpt only ~10% of prostate tissue exhibited MHC I staining, as compared to 30-50% of MHC I^+ tissue in untreated mice (Fig. 3B). The reduction of MHC I^+ expression was antigen specific as transfer of OT-I T cells and infection with WSN-SIIN virus did not affect expression of MHC I expression within the prostates of TRP-SIY mice (Fig. 3B).

In addition to antigen expression, activated T cells within tumors can disrupt tumor stroma, such as $CD31^+$ endothelial cells (18). We determined the levels of tumor vasculature by staining prostate tissue for CD31. Prostate tissue in TRP-SIY mice were well vascularized with clear CD31 staining in both 2C T cell treated and untreated mice (Fig. 3C). No difference in percentage of area that stained positive for CD31 was detected in untreated and treated mice

(Fig. 3D). Together, these data show that 2C T cell response in the prostate tissue leads to a reduction of MHC I expression but not the tumor vasculature.

2C T cell treatment does not alter tumor progression

We next determined whether reduction in antigen expressing prostate cells in treated mice affected tumor progression. To assess tumor progression, H&E stained prostate tissues from 2C treated and untreated mice were blinded and graded for tumor stage (Fig. 4A). At 11 dpt the average tumor grade was the same (1.4) in both treated and age-matched control mice (Fig. 4A). At 35 dpt the average tumor grade in treated and age matched controls was 2.2 and 2.5, respectively. At 50 dpt the average grade was 3.8 for treated mice versus 2.8 for untreated mice. These data suggest that despite clearance of SIY-expressing cells in the TRP-SIY prostates, tumors continue to progress.

TRP-SIY mice were constructed by introducing the β-gal-SIY fusion transgene into the TRAMP mice, which carry the SV40 large T antigen (Tag) transgene. Although both transgenes were driven by the same prostate-specific promoter, the two transgenes were introduced into the mouse genome independently. It is possible that activated 2C T cells eliminated SIY-expressing tumors while those that do not express the SIY antigen grow out after T cell treatment. To test this possibility, we stained untreated TRP-SIY prostate sections for both β-gal and Tag. Although most β-gal and Tag staining overlapped, a significant fraction of prostate area was stained positive for Tag but negative for β-gal (Fig. 4B). Furthermore, to assess the expression of the Tag after 2C T cell treatment we stained treated and untreated prostate sections for Tag (Fig. 4C). At all three time points (11, 35 and 50 dpt), the 2C T cell treatment did not affect the percentage of prostate tissue that stained positive for Tag (Fig. 4D). However, the percentage of Tag-positive area increased over time following 2C treatment, correlating with tumor progression. Taken together, these data suggest that although 2C T cell treatment is effective in eliminating SIY-positive tumor cells, the SIY-negative tumor cells continue to progress.

Discussion

The TRAMP model has been widely used to study prostate cancer immunotherapy. Numerous studies have induced CD8 T cell responses to TRAMP tumor, including clonotypic

$CD8^+$ T cells specific for Tag, HA or SIY epitopes that were engineered to be expressed in the tumor cells, or endogenous CD8 T cells following immunization with a telomerase vaccine. Although antigen-specific CD8 T cells were potently induced in each case, the effect on tumor growth is minimal or transient, as the outgrowth of tumor cells eventually kills the TRAMP mice. The lack of long-lasting efficacy has been attributed to the rapid tolerization of tumor infiltrating T cells by the immunosuppressive tumor environment within TRAMP mice (13, 19, 20). In the current study, by quantifying the level and distribution of responding $CD8^+$ T cells and antigen-bearing tumor cells in the prostate, we show that $CD8^+$ T cells are very effective in eliminating antigen-bearing tumor cells in the prostate. One week after infiltration into the prostate tumor tissue, most of antigen-bearing tumor cells are already eliminated. Notably, aggregates of dead antigen-positive tumor cells are found in the lumen of the prostate gland and in the urethra, suggesting that killed tumor cells are removed from the prostate tissue through the lumen and urethra. The finding that CD8 T cells can effectively eliminate antigen-positive tumor cells in the prostate suggests alternative mechanisms underlying the lack of efficacy on tumor progression and survival of TRAMP mice as observed in many studies.

Our observation of the selection and outgrowth of antigen-negative tumor cells in TRP-SIY mice provides such a mechanism. We show that while SIY-positive tumor cells are eliminated soon after T cell infiltration into the prostate, SIY-negative but Tag^+ cells continue to grow within the tumor bed. The presence of Tag^+ SIY (β-galactosidase)$^-$ tumor cells in TRP-SIY mice prior to T cell treatment further suggests that the outgrowth of Tag^+ SIY^- tumor cells compromised the efficacy of 2C T cell response. This observation is likely an instance of immune-editing where immune responses keep tumors under the control but antigen-negative tumor cells eventually outgrow and escape immune surveillance. Our findings suggest that targeting multiple epitopes in poorly immunogenic tumors may increase the efficacy of immunotherapies. Indeed, in a B16-OVA model where treatment of mice with OT-1 T cells was unable to control tumor growth (6), treatment with both OT-1 and the gp-100 specific Pmel-1 T cells prevented tumor growth (21). Furthermore, our work suggests that targeting of oncogenic drivers of tumor growth with immunotherapy could be a more productive strategy. Previous attempts to use T cells that recognize Tag epitopes in the TRAMP model have provided mixed results with regards to reduction in tumor burden (11, 12). Nevertheless, other models have demonstrated the therapeutic benefit of focusing the immune response toward overexpressed

oncogenes, including Tag (18). The efficacy of combination immunotherapies that target oncogene epitopes and non-oncogene epitopes should be investigated in this and other models.

In addition to antigen loss, cell surface expression of MHC I within the prostate epithelium is reduced in mice 50 dpt. In human melanoma, esophageal, and ovarian cancers MHC I loss is associated with poor prognosis (17, 22, 23). Data from human prostate cancers is mixed with regard to MHC I expression. A study assessing patient samples from varying tumor stages (Gleason stages 6-10) found MHC I expression in all cases (24). A more recent study assessed components of the antigen processing machinery in 59 primary prostate carcinoma and prostate carcinoma cell lines. HLA class I was retained in most tumor lesions, but intracellular antigen processing machinery was not detected in at least 21% tumors (16). Regardless, under steady state conditions MHC I cell surface expression is retained in TRAMP tissues (24). The role of immunotherapies on MHC I expression within prostates of human patients is of interest, as MHC I loss can profoundly influence the efficacy of adaptive immune responses.

The long-term effect on antigen expression and antigen loss variants in many immunotherapeutic modalities is unknown. Clinical trials evaluating ACT in relapsing metastatic melanoma patients demonstrate the emergence of antigen loss variants (25-27). It is unknown how, if at all, antigen expression in different tumor types will be affected by induction of a therapeutic immune response. Indeed, the effect of the FDA approved DC vaccination protocol on antigen expression in primary or relapsing prostate tumors has not been reported. Collectively, these results have important implications for the selection of tumor specific antigens and suggest selection of multiple antigens, including those that drive tumor progression, are attractive targets for generating clinical benefit.

Acknowledgements

We thank Marisha Mikell and the Swanson Biotechnology Core Facility at the Koch Institute for their technical support, members of the Chen and Wittrup Labs for their helpful discussions, and Yin Lu at the Singapore-MIT Alliance for Research and Technology for assistance with processing histology slides.

References

1. Cha E, Fong L. Immunotherapy for Prostate Cancer: Biology and Therapeutic Approaches. J Clin Oncol 2011.
2. Rosenberg SA, Restifo NP, Yang JC, Morgan RA, Dudley ME. Adoptive cell transfer: a clinical path to effective cancer immunotherapy. Nat Rev Cancer 2008;8:299-308.
3. Dudley ME, Wunderlich JR, Yang JC, Sherry RM, Topalian SL, Restifo NP, Royal RE, Kammula U, White DE, Mavroukakis SA, Rogers LJ, Gracia GJ, Jones SA, Mangiameli DP, Pelletier MM, Gea-Banacloche J, Robinson MR, Berman DM, Filie AC, Abati A, Rosenberg SA. Adoptive cell transfer therapy following non-myeloablative but lymphodepleting chemotherapy for the treatment of patients with refractory metastatic melanoma. J Clin Oncol 2005;23:2346-57.
4. Bai XF, Liu JQ, Joshi PS, Wang L, Yin L, Labanowska J, Heerema N, Zheng P, Liu Y. Different lineages of P1A-expressing cancer cells use divergent modes of immune evasion for T-cell adoptive therapy. Cancer Res 2006;66:8241-9.
5. Goldberger O, Volovitz I, Machlenkin A, Vadai E, Tzehoval E, Eisenbach L. Exuberated numbers of tumor-specific T cells result in tumor escape. Cancer Res 2008;68:3450-7.
6. Kaluza KM, Thompson JM, Kottke TJ, Flynn Gilmer HC, Knutson DL, Vile RG. Adoptive T cell therapy promotes the emergence of genomically altered tumor escape variants. Int J Cancer 2012;131:844-54.
7. Sanchez-Perez L, Kottke T, Diaz RM, Ahmed A, Thompson J, Chong H, Melcher A, Holmen S, Daniels G, Vile RG. Potent selection of antigen loss variants of B16 melanoma following inflammatory killing of melanocytes in vivo. Cancer Res 2005;65:2009-17.
8. Landsberg J, Kohlmeyer J, Renn M, Bald T, Rogava M, Cron M, Fatho M, Lennerz V, Wolfel T, Holzel M, Tuting T. Melanomas resist T-cell therapy through inflammation-induced reversible dedifferentiation. Nature 2012;490:412-6.
9. Wada S, Yoshimura K, Hipkiss EL, Harris TJ, Yen HR, Goldberg MV, Grosso JF, Getnet D, Demarzo AM, Netto GJ, Anders R, Pardoll DM, Drake CG. Cyclophosphamide augments antitumor immunity: studies in an autochthonous prostate cancer model. Cancer Res 2009;69:4309-18.
10. Mennuni C, Ugel S, Mori F, Cipriani B, Iezzi M, Pannellini T, Lazzaro D, Ciliberto G, La Monica N, Zanovello P, Bronte V, Scarselli E. Preventive vaccination with telomerase controls tumor growth in genetically engineered and carcinogen-induced mouse models of cancer. Cancer Res 2008;68:9865-74.
11. Anderson MJ, Shafer-Weaver K, Greenberg NM, Hurwitz AA. Tolerization of tumor-specific T cells despite efficient initial priming in a primary murine model of prostate cancer. J Immunol 2007;178:1268-76.
12. Shafer-Weaver KA, Watkins SK, Anderson MJ, Draper LJ, Malyguine A, Alvord WG, Greenberg NM, Hurwitz AA. Immunity to murine prostatic tumors: continuous provision of T-cell help prevents CD8 T-cell tolerance and activates tumor-infiltrating dendritic cells. Cancer Res 2009;69:6256-64.
13. Bai A, Higham E, Eisen HN, Wittrup KD, Chen J. Rapid tolerization of virus-activated tumor-specific CD8+ T cells in prostate tumors of TRAMP mice. Proc Natl Acad Sci U S A 2008;105:13003-8.
14. Olurinde MO, Shen CH, Drake A, Bai A, Chen J. Persistence of tumor-infiltrating CD8 T cells is tumor-dependent but antigen-independent. Cell Mol Immunol 2011.

15. Bak SP, Barnkob MS, Bai A, Higham EM, Wittrup KD, Chen J. Differential requirement for CD70 and CD80/CD86 in dendritic cell-mediated activation of tumor-tolerized CD8 T cells. J Immunol 2012;189:1708-16.
16. Seliger B, Stoehr R, Handke D, Mueller A, Ferrone S, Wullich B, Tannapfel A, Hofstaedter F, Hartmann A. Association of HLA class I antigen abnormalities with disease progression and early recurrence in prostate cancer. Cancer Immunol Immunother 2010;59:529-40.
17. Kageshita T, Hirai S, Ono T, Hicklin DJ, Ferrone S. Down-regulation of HLA class I antigen-processing molecules in malignant melanoma: association with disease progression. Am J Pathol 1999;154:745-54.
18. Anders K, Buschow C, Herrmann A, Milojkovic A, Loddenkemper C, Kammertoens T, Daniel P, Yu H, Charo J, Blankenstein T. Oncogene-targeting T cells reject large tumors while oncogene inactivation selects escape variants in mouse models of cancer. Cancer Cell 2011;20:755-67.
19. Watkins SK, Zhu Z, Riboldi E, Shafer-Weaver KA, Stagliano KE, Sklavos MM, Ambs S, Yagita H, Hurwitz AA. FOXO3 programs tumor-associated DCs to become tolerogenic in human and murine prostate cancer. J Clin Invest 2011;121:1361-72.
20. Donkor MK, Sarkar A, Savage PA, Franklin RA, Johnson LK, Jungbluth AA, Allison JP, Li MO. T cell surveillance of oncogene-induced prostate cancer is impeded by T cell-derived TGF-beta1 cytokine. Immunity 2011;35:123-34.
21. Kaluza KM, Kottke T, Diaz RM, Rommelfanger D, Thompson J, Vile R. Adoptive transfer of cytotoxic T lymphocytes targeting two different antigens limits antigen loss and tumor escape. Hum Gene Ther 2012;23:1054-64.
22. Mizukami Y, Kono K, Maruyama T, Watanabe M, Kawaguchi Y, Kamimura K, Fujii H. Downregulation of HLA Class I molecules in the tumour is associated with a poor prognosis in patients with oesophageal squamous cell carcinoma. Br J Cancer 2008;99:1462-7.
23. Han LY, Fletcher MS, Urbauer DL, Mueller P, Landen CN, Kamat AA, Lin YG, Merritt WM, Spannuth WA, Deavers MT, De Geest K, Gershenson DM, Lutgendorf SK, Ferrone S, Sood AK. HLA class I antigen processing machinery component expression and intratumoral T-Cell infiltrate as independent prognostic markers in ovarian carcinoma. Clin Cancer Res 2008;14:3372-9.
24. Nanda NK, Birch L, Greenberg NM, Prins GS. MHC class I and class II molecules are expressed in both human and mouse prostate tumor microenvironment. Prostate 2006;66:1275-84.
25. Thurner B, Haendle I, Roder C, Dieckmann D, Keikavoussi P, Jonuleit H, Bender A, Maczek C, Schreiner D, von den Driesch P, Brocker EB, Steinman RM, Enk A, Kampgen E, Schuler G. Vaccination with mage-3A1 peptide-pulsed mature, monocyte-derived dendritic cells expands specific cytotoxic T cells and induces regression of some metastases in advanced stage IV melanoma. J Exp Med 1999;190:1669-78.
26. Maeurer MJ, Gollin SM, Martin D, Swaney W, Bryant J, Castelli C, Robbins P, Parmiani G, Storkus WJ, Lotze MT. Tumor escape from immune recognition: lethal recurrent melanoma in a patient associated with downregulation of the peptide transporter protein TAP-1 and loss of expression of the immunodominant MART-1/Melan-A antigen. J Clin Invest 1996;98:1633-41.
27. Yee C, Thompson JA, Byrd D, Riddell SR, Roche P, Celis E, Greenberg PD. Adoptive T cell therapy using antigen-specific CD8+ T cell clones for the treatment of patients with

metastatic melanoma: in vivo persistence, migration, and antitumor effect of transferred T cells. Proc Natl Acad Sci U S A 2002;99:16168-73.

Figure Legends

Figure 1. Prostate infiltrating T cells gradually lose contact with antigen-expressing tumor cells. 2C T cells were adoptively transferred into TRP-SIY mice followed by WSN-SIY infection. Eleven, 35 and 50 dpt, prostate sections were stained with anti-Thy1.1 (brown), X-gal (blue) and eosin (red). A. Representative stains for Thy1.1 (left), isotype control (center) and β-gal (right) of prostate sections of TRP-SIY mice 11 dpt. Scale bars, 100μm. B-D. The areas of Thy1.1 and β-gal staining were quantified as described in the Materials and Methods. Shown are percentages (mean ± SD) of area within the prostate tissue that stain positive for Thy1.1$^+$ 2C T cells at indicated time point (B). Representative images of Thy1.1 and β-gal stains of prostate sections of a mouse 11 dpt (C). Thy1.1 staining was classified as either in contact with β-gal$^+$ cells (contact, highlighted in yellow), within a prostate gland containing β-gal$^+$ cells (β-gal$^+$ gland), within a prostate gland that does not contain β-gal staining (β-gal$^-$ gland), in the interglandular interstitial space (interstitial space), or within the lumen of the prostate gland (lumen). The boxed areas are shown in higher magnifications. Scale bars, 100μm and 30μm in low and high magnifications, respectively. The areas of Thy1.1 stain in each category were quantified and shown as percentages of total Thy1.1$^+$ area (mean ± SD) (D). The numbers of mice analyzed in each group for B and D are indicated.

Figure 2. Antigen positive cells are lost from 2C T cell-treated TRP-SIY prostates. Prostate sections from age-matched untreated and treated mice were stained for β-gal, Thy1.1 and eosin and both the β-gal and Thy1.1-stained areas were quantified. A. Representative images of staining for β-gal (blue) and Thy1.1 (brown) counterstained with eosin (red) of untreated mice and treated mice 11, 35 and 50 dpt. B. Percentages (mean ± SD) of β-gal$^+$ areas in the prostate section of untreated (black) and treated (open) mice at the indicated dpt. Some mice were transferred with OT-1 T cells and infected with WSN-SIIN virus and the percentage of β-gal$^+$ area was quantified 50 dpt (dashed bar). The numbers of mice in each group are indicated. C. β-gal staining was classified as localizing to the gland (blue), lumen (grey) or interstitial space

(dash) of the prostate sections from the same group of mice treated in B and expressed as an average percentage of total β-gal staining. D. Representative β-gal (left) ad H&E (left) staining of consecutive prostate sections from a mouse 11 dpt. Scale bars in both A and D, 100μm. ***p value of < 0.001 as compared to untreated group. n.s., not significant.

Figure 3. MHC class I expression is reduced in 2C T cell treated prostates. A and B. Mice were treated as in Figure 2 and the 2C T cell treated prostate tissues and aged matched untreated control tissues (Untreated) were stained for MHC I (dark brown) and hematoxylin (light brown) and quantified. Representative staining of MHC I and hematoxylin from TRP-SIY prostate tissue at indicated time point with or without treatment (A). Percentages of area within the prostate tissue staining positive for MHC class I in 2C T cell treated (triangles), untreated (circles), or TRP-SIY mice receiving OT-1 T cells activated with WSN-SIIN virus (diamonds) at indicated time points (B). Each symbol represents one mouse. C and D. Prostate sections from age-matched untreated and 2C treated mice were stained for CD31 and eosin and the stained areas were quantified. Representative stains of CD31 (brown) and eosin (red) of untreated mice and treated mice 11, 35 and 50 dpt (C). Percentages (mean ± SD) of $CD31^+$ areas in the prostate section of untreated (circles) and 2C treated (triangles) mice at the indicated dpt (D). Scale bars in A and C, 100μm.

Figure 4. 2C T cell treatment does not affect tumor progression. A. Mice were treated as in Figure 2, prostate sections from both 2C T cell treated and age matched untreated mice were stained with H&E and graded (0, normal tissue; 1, proliferation with no invasion; 2, early invasion; 3, clear-cut invasion; 4, total replacement of organ). Shown are tumor grade at 11, 35, and 50 dpt. Each symbol represents one mouse. The numbers in parentheses indicate the average of tumor grade at each time point. B. Prostate sections from untreated TRP-SIY mice were stained for β-gal (blue), Tag (brown) and eosin (red). Representative images are shown for prostate sections from mice at 16 weeks of age. C and D. Mice were treated as in Figure 2, prostate sections from both 2C T cell treated and age matched untreated mice were stained for Tag (dark brown) and eosin (red). Shown are representative Tag staining of prostate sections from 2C treated mice at 11, 35 and 50 dpt and age-matched untreated mice (C). Percentages (mean ± SD) of Tag^+ areas in the prostate section of untreated and 2C treated mice at the

indicated dpt (D). Scale bars in B and C: 100μm.

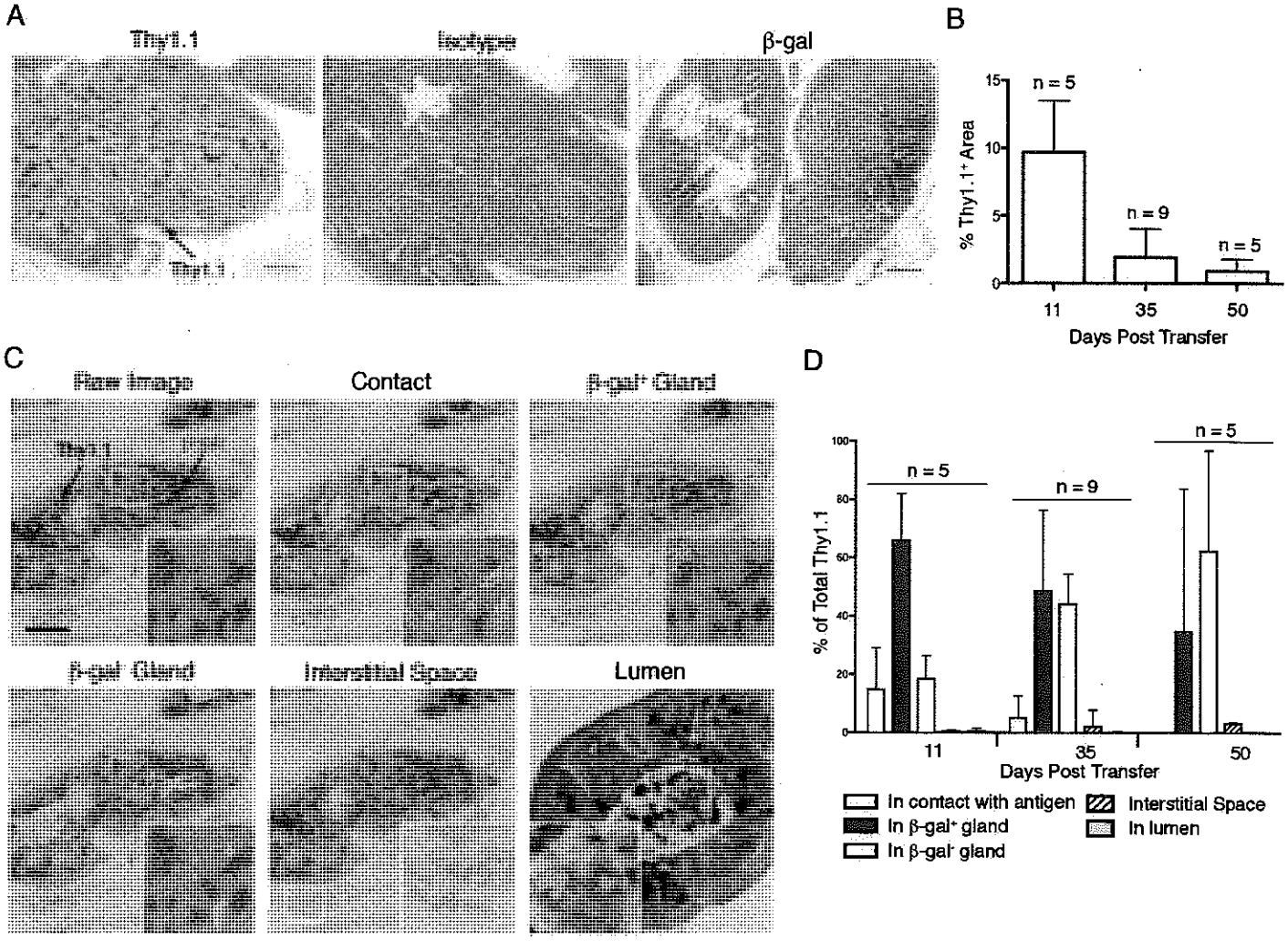
A
Thy1.1
Isotype
β-gal
B
% Thy1.1+ Area
n = 5
n = 9
n = 5
11
35
50
Days Post Transfer
C
Raw Image
Contact
β-gal+ Gland
β-gal- Gland
Interstitial Space
Lumen
D
% of Total Thy1.1
n = 5
n = 9
n = 5
11
35
50
Days Post Transfer
In contact with antigen
In β-gal+ gland
In β-gal- gland
Interstitial Space
In lumen

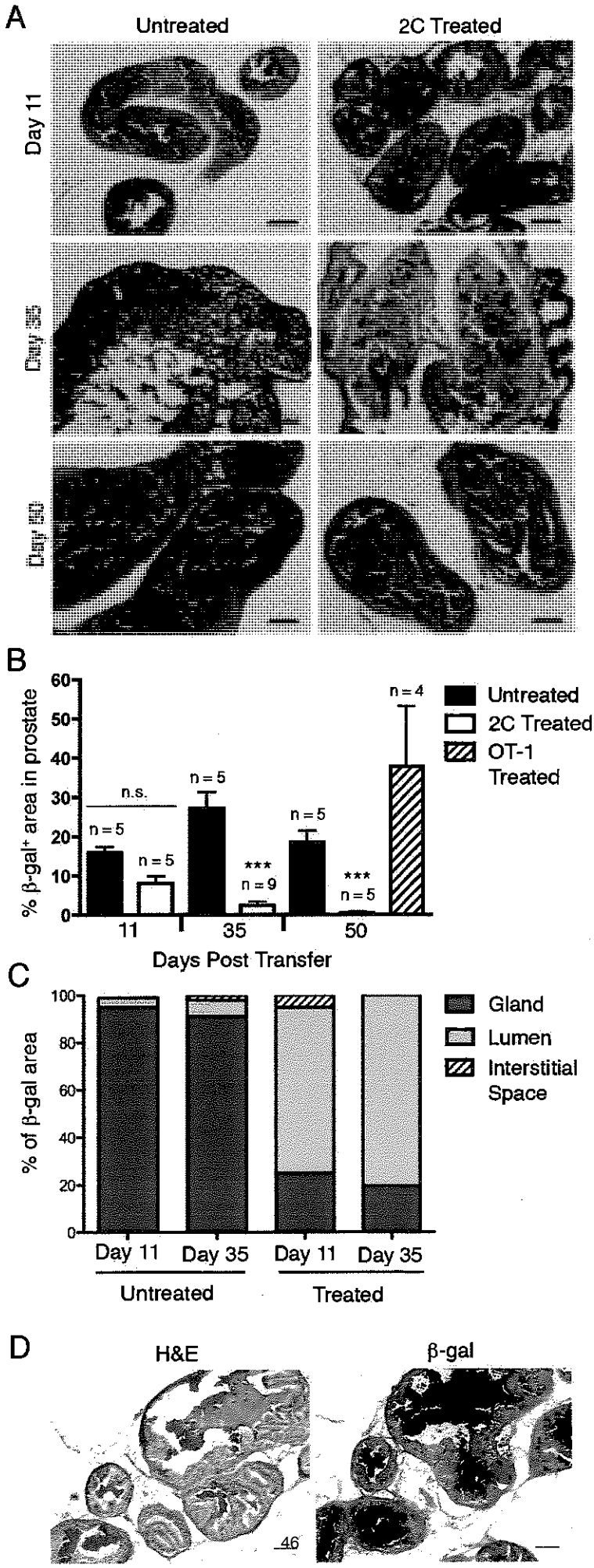
A
Untreated
2C Treated
Day 11
Day 35
Day 50
B
% β-gal+ area in prostate
60
50
40
30
20
10
0
n.s.
n = 5
n = 5
n = 5
***
n = 9
n = 5
***
n = 5
n = 4
11
35
50
Days Post Transfer
Untreated
2C Treated
OT-1 Treated
C
% of β-gal area
100
80
60
40
20
0
Day 11
Day 35
Day 11
Day 35
Untreated
Treated
Gland
Lumen
Interstitial Space
D
H&E
β-gal

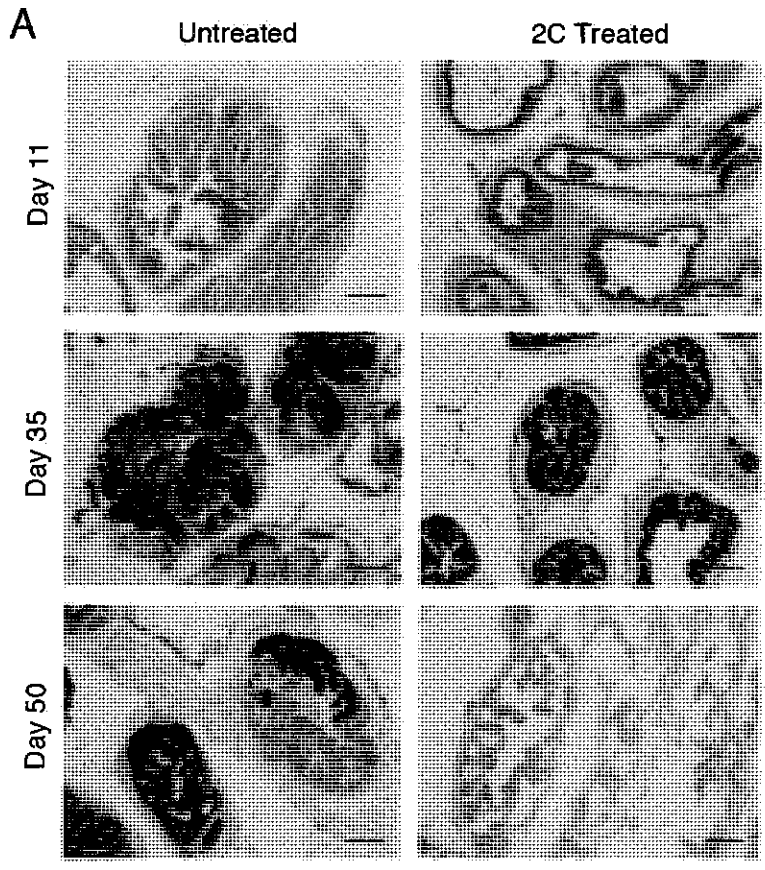
A
Untreated
2C Treated
Day 11
Day 35
Day 50

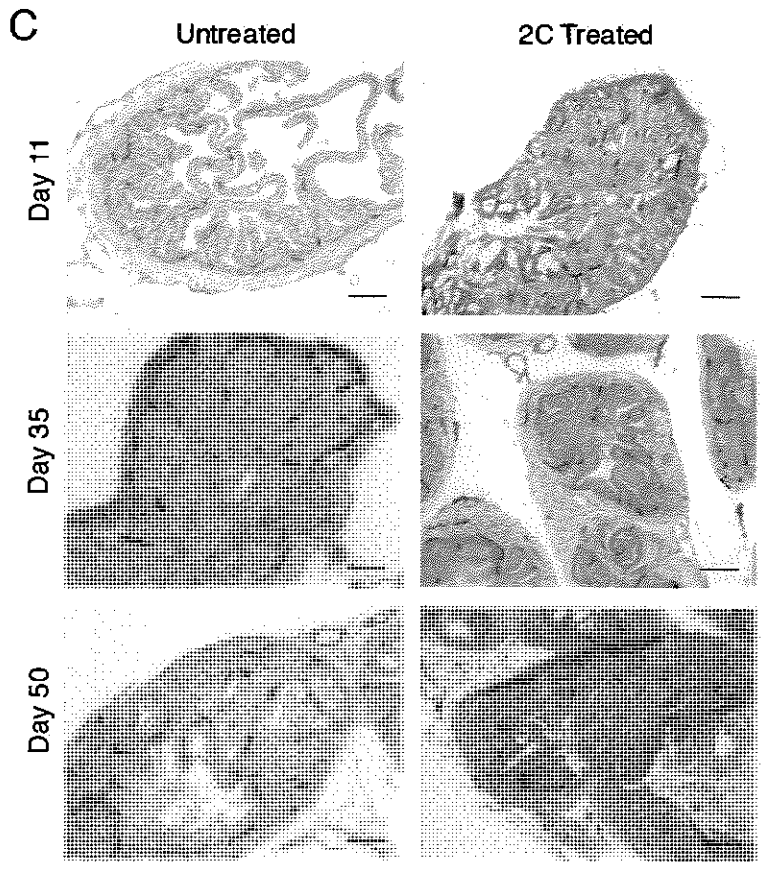
C
Untreated
2C Treated
Day 11
Day 35
Day 50

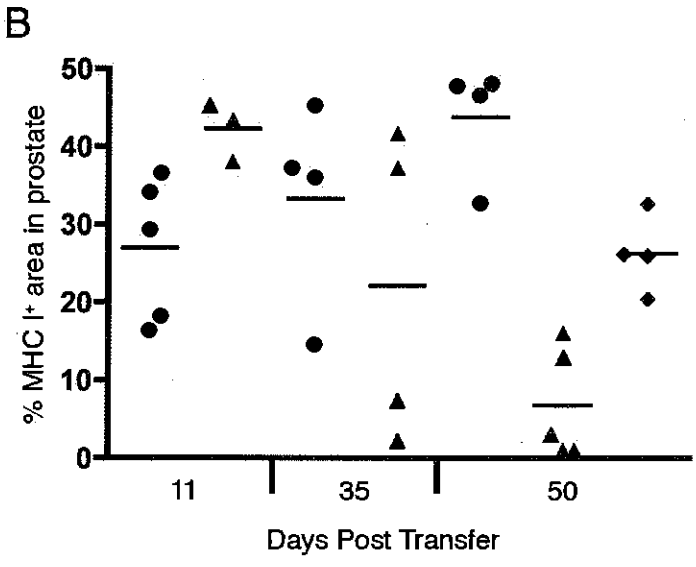
B
% MHC I+ area in prostate
50
40
30
20
10
0
11
35
50
Days Post Transfer

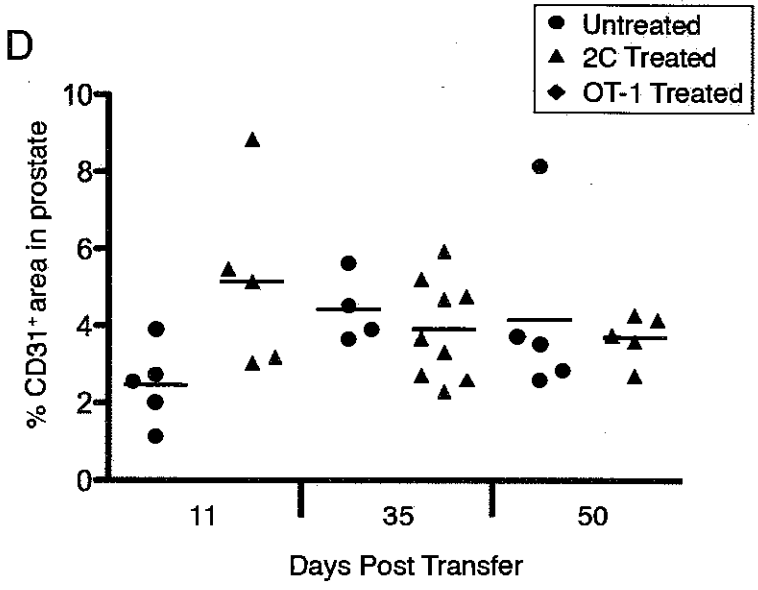
D
Untreated
2C Treated
OT-1 Treated
% CD31+ area in prostate
10
8
6
4
2
0
11
35
50
Days Post Transfer

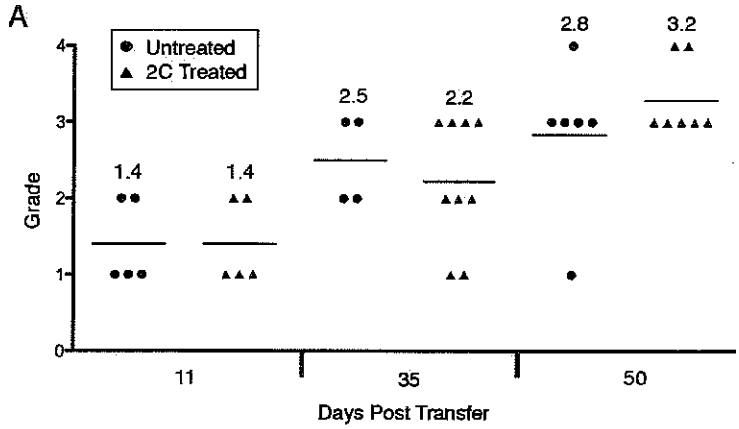
A
Untreated
2C Treated
Grade
Days Post Transfer
1.4
1.4
2.5
2.2
2.8
3.2
11
35
50

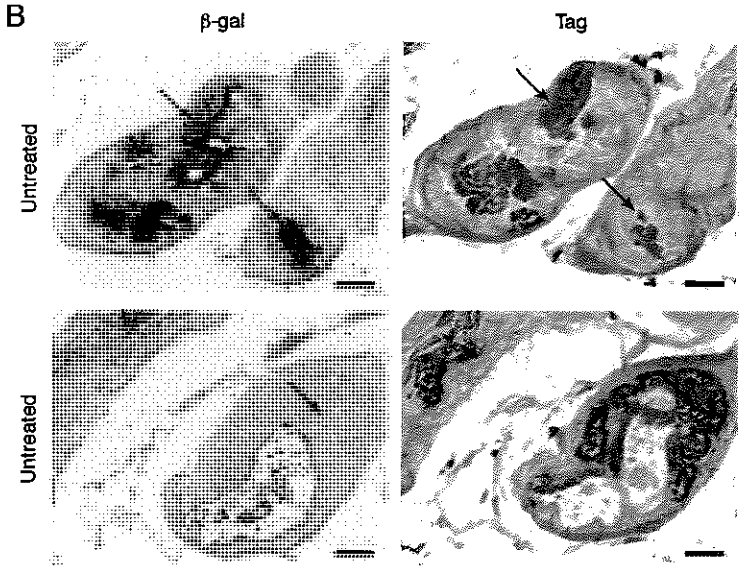
B
β-gal
Tag
Untreated
Untreated

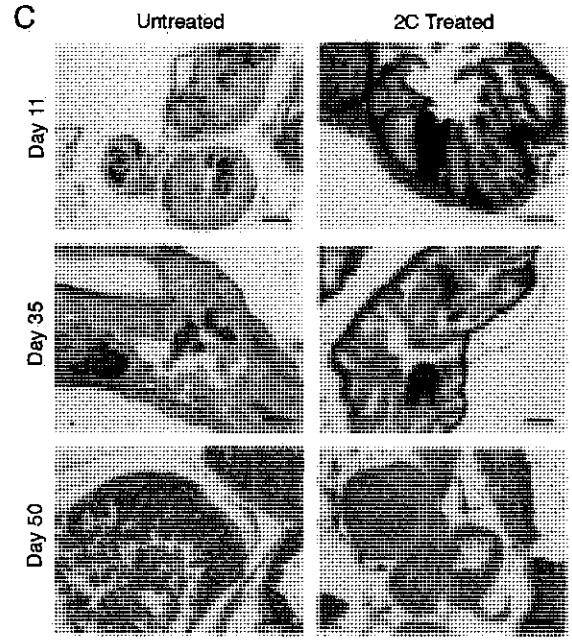
C
Untreated
2C Treated
Day 11
Day 35
Day 50

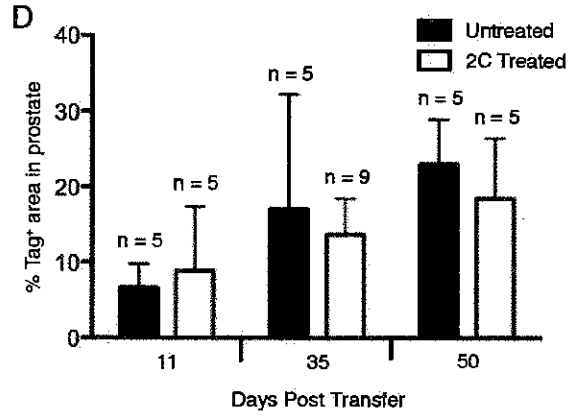
D
Untreated
2C Treated
% Tag+ area in prostate
n = 5
n = 5
n = 5
n = 9
n = 5
n = 5
Days Post Transfer